2017

# The Effect of Morphology on Reflectance in Silicon Nanowires Grown by Electroless Etching

Victor Velez
*University of Central Florida*

# THE EFFECT OF MORPHOLOGY ON REFLECTANCE IN SILICON NANOWIRES GROWN BY ELECTROLESS ETCHING

by

VICTOR HUGO VELEZ
B.S.E.E. Universidad Autonoma de Occidente, 2000
M.S.C.E. University of Central Florida, 2009

A dissertation submitted in partial fulfillment of the requirements
for the degree of Doctor of Philosophy
in the Department of Electrical Engineering and Computer Science
in the College of Engineering and Computer Science
at the University of Central Florida
Orlando, Florida

Summer Term
2017

Major Professor: Kalpathy B. Sundaram

# ABSTRACT

The strong light trapping properties of Silicon Nanowires have attracted much interest in the past few years for the conversion of sun energy into conventional electricity. Studies have been completed for many researchers to reduce the cost of fabrication and reflectance of solar light in these nanostructures to make a cheaper and more efficient solar cell technology by using less equipment for fabrication and employing different materials and solution concentrations. Silver, a conducting and stable metal is used these days as a precursor to react with silicon and then form the nanowires. Its adequate selection of solution concentration for a size of silicon substrate and the treatment for post-cleaning of silver dendrites make it a viable method among the others. It is an aim of this research to obtain significant low reflectance across the visible solar light range. Detailed concentration, fabrication and reflectance studies is carried out on silicon wafer in order to expand knowledge and understanding.

In this study, electroless etching technique has been used as the growth mechanism of SiNWs at room temperature. Optimum ratios of solution concentration and duration for different sizes of exposed area to grow tall silicon nanowires derived from experimentation are presented. Surface imaging of the structures and dimension of length and diameter have been determined by Scanner Electron Microscopy (SEM) and the reflectance in the optical range in silicon nanowires has been make using UV-Visible Spectrophotometer.

Dedicated to my beloved parents and family

# ACKNOWLEDGMENTS

I would like to thank my advisor, Dr. Kalpathy B Sundaram, for the opportunity he gave me to pursue my dream to complete my Ph.D. degree, for his commitment and guidance to help me discover and polish skills that were a challenge is the past. His advice, has been eminently meaningful to my experience as a graduate student and as a person. Also, I would like to thank Dr. Jiann S Yuan, Dr. Reza Abdolvand, Dr. Vikram J Kapoor, and Dr. Aravinda Kar for serving on my thesis committee and their support throughout my years at UCF.

I would like to acknowledge thin films lab facility and the materials characterization facility (MCF) at the advanced materials processing and analysis center (AMPAC) at the University of Central Florida (UCF) for their constant support and collaboration when guidance was necessary in the laboratory. Also, I would like to thank the Student Government Association (SGA) at UCF and the Electrochemical Society for their funding assistance and great technical contribution respectively obtained when attended technical conferences to present publication. Special thanks to Dr. Robert G. Mertens and Dr. Sacharia Albin for serving as source of inspiration and encouragement throughout my research at UCF.

I would like to thank my parents Mr. Rubiel Velez and Ms. Isabel Restrepo for believe in me and their enormous and uninterrupted motivation during my graduate degree. Also I would like to thank my uncles Adolfo Arbelaez and Guillermo Restrepo for encouraging me and value my great effort to persist in my goal.

# TABLE OF CONTENTS

LIST OF FIGURES ............................................................ viii

LIST OF TABLES ............................................................ xi

LIST OF ACRONYMS/ABBREVIATIONS ............................................................ xii

CHAPTER 1: GENERAL INTRODUCTION ............................................................ 1

CHAPTER 2: LITERATURE REVIEW ............................................................ 5

CHAPTER 3: EXPERIMENTS AND DESIGNS ............................................................ 10

3.1: Investigation on the Reflectance Properties on Silicon Nanowires Grown by Electroless Etching............................................................ 11

3.2: Post cleaning effects on silicon nanowires grown by electroless etching. .................. 11

3.3: Area Effect of Reflectance in Silicon Nanowires Grown by Electroless Etching. ...... 12

3.4: Agglomeration in Porous Silicon Prepared From Si-Nanowire Structures ................. 12

3.5: Morphology in Porous Silicon Prepared From Si-Nanowires Grown by Electroless Etching. ............................................................ 13

CHAPTER 4: RESULT AND DISCUSSION ............................................................ 15

4.1: Investigation on the Reflectance Properties on Silicon Nanowires Grown by Electroless Etching............................................................ 15

4.2: Post cleaning effects on silicon nanowires grown by electroless etching. .................. 20

4.3: Area Effect of Reflectance in Silicon Nanowires Grown by Electroless Etching. ...... 24

4.4: Agglomeration in Porous Silicon Prepared From Si-Nanowire Structures ................. 29

4.5: Morphology in Porous Silicon Prepared From Si-Nanowires Grown by Electroless Etching. ........................................................................................................................ 32

CONCLUSIONS......................................................................................................... 39

REFERENCES ........................................................................................................... 41

# LIST OF FIGURES

Figure 1: Reflectance on a polished planar silicon ........................................................................ 6

Figure 2: Diagram of the used anode electrolytic etching circuit to reduce the quantum confinement of the SiNWs. ........................................................................................... 13

Figure 3: SEM pictures of the SiNWs grown using the concentration of HF 16.66% and $AgNO_3$ 23.33% a) 15 min b) 30 min c) 45 min and d) 60 min. ............................................................ 16

Figure 4: SEM pictures of the SiNWs grown using the concentration of HF 20% and $AgNO_3$ 20% a) 15 min b) 30 min c) 45 min and d) 60 min. ..................................................................... 16

Figure 5: SEM pictures of the SiNWs grown using the concentration of HF 23.33% and $AgNO_3$ 16.66% a) 15 min b) 30 min c) 45 min and d) 60 min. ............................................................ 17

Figure 6: Trend lines of SiNW arrays lengths for solutions 1, 2 and 3 grown at different periods of time; 15 min, 30 min, 45 min and 60 min. ................................................................... 19

Figure 7: Reflectance plots as a function of wavelength a) HF 16.66% and $AgNO_3$ 23.33%, b) HF 20% and $AgNO_3$ 20% and c) HF 23.33% and $AgNO_3$ 16.66%. ............................................ 20

Figure 8: (a) 45$^o$ cross-sectional and (b) top view SEM pictures of SiNWs cleaned in an unstirred solution of 20% $HNO_3$ and 80% DI water for 25 minutes. ...................................................... 21

Figure 9: (a-d) 45$^o$ tilted cross-sectional and (e-h) top view SEM pictures of SiNWs cleaned in a stirred solution of 20% $HNO_3$ and 80% DI water for 25 minutes at (a, e) 60, (b, f) 300, (c, g) 550 and (d, h) 800 rpm. ................................................................................................ 22

Figure 10: Reflectance plots as a function of wavelength in the visible region for silicon nanowires samples stirred and unstirred in diluted nitric acid solution. ...................................... 23
Figure 11: SEM pictures of the SiNWs grown using the concentration of HF 26.666 % and $AgNO_3$ 13.334 % grown in a silicon wafer size surface of (a) 2 $cm^2$ (b) 4 $cm^2$ (c) 8 $cm^2$ and (d) 16 $cm^2$. ........................................................................................................................ 24
Figure 12: SEM pictures of the SiNWs grown using the concentration of HF 23.33 % and $AgNO_3$ 16.66 % grown in a silicon wafer size surface of (a) 2 $cm^2$ (b) 4 $cm^2$ (c) 8 $cm^2$ and (d) 16 $cm^2$. ........................................................................................................................ 25
Figure 13: SEM pictures of the SiNWs grown using the concentration of HF 20 % and $AgNO_3$ 20 % grown in a silicon wafer size surface of (a) 2 $cm^2$ (b) 4 $cm^2$ (c) 8 $cm^2$ and (d) 16 $cm^2$. ..... 25
Figure 14: SiNW arrays length as a function of silicon surface areas for different etching solution concentrations. ........................................................................................................... 27
Figure 15: Electroless etching process during SiNWs fabrication. ............................................. 28
Figure 16: Reflectance plots of SiNWs prepared with different substrate surface sizes (2, 4, 8 and 16 $cm^2$) for varies concentrations of, (a) HF is 26.66% and $AgNO_3$ is 13.33%, (b) HF is 23.33% and $AgNO_3$ is 16.66% and (c) HF is 20% and $AgNO_3$ is 20%.................................................... 29
Figure 17: 3D photoluminescence spectrum when ultraviolet light is exposed on porous SiNWs fabricated in a solution concentration containing a) 33.33% HF and 66.66% $C_2H_6O$ for 15 min etching time at 25 mA, and b) 33.33% HF and 66.66% $C_2H_6O$ for 15 min etching time at 250 mA........................................................................................................................... 31
Figure 18: Reflectance analysis across the visible spectrum of SiNWs grown using the electroless technique and porous SiNWs fabricated from prepared electroless SiNWs............... 32

Figure 19: Cross-section SEM image showing the top part of porous silicon nanowires structures when prepared SiNW arrays are etched in an electrolytic solution at room temperature, and an electric current of 30mA for 15 minutes. 34

Figure 20 temperature: Cross-section SEM imagens of porous SiNWs prepared in an electrolytic solution at room and with a current of 30mA for 15 minutes containing a) 80% HF and 20% $C_2H_6O$, b) 60% HF and 40% $C_2H_6O$, c) 40% HF and 60% $C_2H_6O$ and d) 20% HF and 80% $C_2H_6O$. 34

Figure 21: Reflectance analysis in SiNWs and porous SiNWs across the visible spectrum. 35

Figure 22: Reflectance analysis across the visible spectrum of SiNWs grown by electroless etching at different temperatures during 15 minutes in a solution bath with concentration of 20% HF, 20% $AgNO_3$, and 60% DI $H_2O$. 37

Figure 23: Trend lines of SiNW arrays lengths grown by electroless etching at temperatures of 25°C, 35°C, 45°C, 55°C during 15 minutes in a solution bath with concentration of 20% HF, 20% $AgNO_3$, and 60% DI $H_2O$. 38

Figure 24: Cross sectional SEM images of SiNW arrays obtained by electroless etching during 15 minutes conducted at (a) 25°C (b) 35°C (c) 45°C (d) 55°C. 38

# LIST OF TABLES

Table 1: Concentrations of Solutions for 15, 30, 45 and 60 minutes etching time....................... 11

Table 2: Concentrations of Etching Solutions for area effect of reflectance in SiNWs ............... 12

Table 3: Etching duration and SiNW array lengths for each solution concentration ................... 17

Table 4: Reflectance across the visual spectrum cleaned in unstirred and stirred nitric acid solutions. ........................................................................................................................ 21

Table 5: Reflectance across the visual spectrum in SiNWs grown using the electroless technique and porous SiNWs fabricated from prepared electroless SiNWs. ............................................... 32

Table 6: Lengths and diameters of SiNW and porous SiNW arrays grown using different solutions. ........................................................................................................................ 35

Table 7: SiNWs arrays lengths measured at different temperatures............................................. 37

# LIST OF ACRONYMS/ABBREVIATIONS

1D – One dimensional

°C - Degrees centigrade/Celsius

Ω-cm - Ohm-centimeter

μm - microns

Ag - Silver

$Ag^+$ - Silver positive ion

$Ag_2O$ - Silver oxide

$AgNO_3$ - Silver nitrate

AgOH - Silver hydroxide

AM1.5 - air mass 1.5

(aq) - Aqueous

AR - Antireflective

BOE - Buffered oxide etch

cm - centimeters

$cm^2$ - square centimeters

$C_2H_6O$ - Ethanol

CVD - Chemical vapor deposition

d - Average diameter of the SiNWs

DI $H_2O$ - Deionized water

DRIE – Direct reactive ion etching

EDS - Energy-dispersive X-ray spectroscopy

EE – Electroless etching

eV – Electron volts

$H_2O_2$ - Hydrogen peroxide

HF - Hydrofluoric acid

$HNO_3$ - Nitric acid

$H_{NW}$ - average height of the SiNWs

M - Molar, molarity, moles

mA – milliamps

mg - milligrams

min. - minutes

ml - milliliters

$mm^2$ - square millimeters

$N_2$ - Nitrogen (gaseous)

nm - nanometers

NWs - Nanowires

PR – photoresist

rpm – revolutions per minute

(s) - solid

SEM - scanning electron microscope

Si - Silicon

$SiF_6^{2-}$ - Silicon hexafluoride ion

Si-ICs - Silicon integrated circuits

SiNW - Silicon nanowire

SiNWs - Silicon nanowires

t - Thickness (Si wafer)

T - Temperature in Kelvin

UV - ultraviolet

VLS - vapor-liquid-solid

W - Watts

# CHAPTER 1: INTRODUCTION

The response to the growing demand for clean sources of energy in the last decades to reduce global warming, mitigate greenhouse gas emission, enhance sustainability, and keep fossil fuel prices lower has focused researchers to develop alternative renewable technologies. Sunlight along with biomass, wind power and hydropower electricity is one of most accessible renewable energies on the planet. The large quantity of solar energy available makes this renewable power source highly attractive. However, a small fraction of sunlight is used to be converted in solar power, among which, only a 63% of the solar radiation is absorbed for solar panels. The rest of the solar radiation is reflected or lost due to solar cell efficiency issues.

Several studies have been conducted to increase the efficiency of photovoltaic (PV) solar cells by decreasing the reflection losses. Different techniques have been used to reduce the reflection loss from active components of the system including solar cell glass surface treatment and application of various types of coating. These coatings reduce the refractive index at the glass surface of solar cells by applying a nanoporous silica layer. Coating solutions become to be a prominent way to increase the solar light absorption in PV systems, reduce cost of fabrication and improve mechanical stability and bandwidth. However, these techniques just reduce the reflection loss up to 15%.

Recently, different techniques have been used for fabrication of silicon nanowire-based solar cells to improve the absorption of solar radiation. The effects of wire length, diameter, color and wire pitch in silicon nanowire arrays have been investigated by researchers due to the strong broadband and very high optical light absorption. However, the cost of fabrication and the

different techniques applied to grow nanowires with antireflective properties have opened the interest to study the facts that affect the absorption of the solar light in these nanostructures.

In the present dissertation, optical reflectance studies were performed in SiNWs prepared controlling different parameters to improve the absorption of the optical light in the nanostructures.

Chapter 2 is intended to provide the reader with a comprehensive background on current state of the art in the literature pertaining to study of silicon nanowires structures. An overview of recent accomplishments, opportunities and challenges of this structures as a sunlight absorption device for modern applications in PV solar cells has been systematically studied.

Chapter 3 discusses the experimental procedures and techniques used in fabrication of the SiNWs. Material and optical characterization techniques used in the study of these nanostructures have been outlined.

Chapter 4 provides five sections including description and details of experiments to show improvements in reflectance SiNWs. In the first section, the study shows the optical reflectance in silicon nanowires as a function of both etching solution concentration and etching timings. Three different etching solution concentration were used to grow SiNWs with four different durations of etching of timings. These synthesized structures absorbed up to 98.8 % of incident radiation in the same wavelength range. This result is much better than that of polished planar silicon as they absorbed maximum 65% of the radiation in the same wavelength range analyzed for SiNWs. This decrease in reflectance suggests that SiNWs could provide increased photon absorption and could enhance the carrier collection in solar cells and other optoelectronic devices.

In the section 2, optical reflectance studies were performed in SiNWs prepared under various cleaning procedures to remove the silver dendrites. No previous work has been reported on the systematic cleaning procedures of SiNWs after the preparation. This cleaning procedure in SiNWs is done by dipping samples of these prepared nanostructures in a diluted nitric acid solution under different stirring rates.

In section 3, the optical reflectance in SiNWs as a function of both etching solution concentration and size of the silicon wafers are reported. Previously no studies have been reported on the substrate area effects on the reflectance properties of SiNWs. Three different etching solution concentrations were used to grow SiNWs using four different sizes of the silicon substrates.

In section 4, the study focuses on the photoluminescence in SiNWs as a function of etching time, electrical current and anode electrolytic concentration. The electrolytic procedure in SiNWs is done by dipping samples of these prepared nanostructures in a solution of ethanol ($C_2H_6O$) and diluted hydrofluoric acid (HF). Subsequently, the optical reflectance properties were studied in these samples.

In section 5, changes in the morphology of porous SiNWs are reported. It may be the result of increasing the concentration of the oxidizer when prepared silicon nanowires are etched in an electrolytic solution. Further changes are achieved in the diameter and length when the prepared electroless SiNW arrays are etched in an anodic solution to obtain porous silicon nanowires. They have a tendency to become thin and collapse each other forming bunches on the surface. Bunched silicon nanowires structures may be desirable for optical and luminescence applications.

In Section 6, is shown that the optical reflectance in SiNWs fabricated at 25°C by the electroless technique may be lower than when these nanostructures are prepared at higher temperatures. It shows that optical reflectivity can be decreased down to 2.2% for most of the visual spectrum when these nanostructure are fabricated at 25°C. Optical reflectance analysis on SiNWs fabricated at different temperatures are reported.

Chapter 5 summarizes this research major conclusions and recommendations for effecting the needed changes in order to achieve better results to reduce the light reflectance in SiNWs. These conclusions and recommendations are based on the evidence reviewed in this dissertation and on the committee members' collective expertise.

# CHAPTER 2: LITERATURE REVIEW

Silicon structures dates back to the late 1950's when Treuting and Arnold reported the first synthesis of <111> oriented silicon filament crystals commonly named Si whiskers or nanorods in reference to the macroscopy dimensions of the diameter of these structures [1-3]. Then, Morales and Lieber reported synthesizes of silicon structures at nanoscopic dimensions in mid 1990s [4, 5]. Nowadays, structures with diameters of less than 100 nm are considered SiNWs nanowires. Silicon is still the most important semiconducting material for the semiconductor industry due to the narrow and tunable band gap characteristics for applications in photonics and microelectronics [6, 7]. Beside these properties on Si, the antireflective nature appearance of SINWs offer efficient charge transport and controllable optical properties useful in an extensive range of fields including field effect transistors [8, 9], thermoelectric systems [10, 11], bio/chemical sensors [12], photodetectors [13], lithium batteries [14, 15], light emitting diodes [16] and solar cells [17, 18].

Many of the techniques and processes used in the fabrication of silicon integrated circuits (Si-ICs) can also be applied to the manipulation and production of silicon nanowires. The optical reflection response at the surface of the silicon substrate for the range of the solar spectrum is very important for photovoltaic applications.

Polished planar silicon optical reflectance was measured in our laboratory with the angle of incidence on the wafer of 8 degrees at room temperature. It reaches 65% reflectance at a wavelength of 380 nm and between 35% and 44% reflectance in the range of 800 and 454 nm respectively, as shown in Figure 1. These elevated percentages of reflectance indicate high

refractive index of silicon which determines how much light is bent, or refracted, when entering the surface of the polished silicon wafer.  Reducing the reflection of polished monocrystalline silicon has become an area of active research with the goal of improving the efficiency in photovoltaic devices. Currently, antireflective (AR) coating layers are applied on solar cells made of polished monocrystalline silicon (polysilicon) to reduce reflectance. But, problems such as thermal mismatch, material selection, adhesiveness and stability affected the broadband and angle-independent antireflection coating in solar cells.

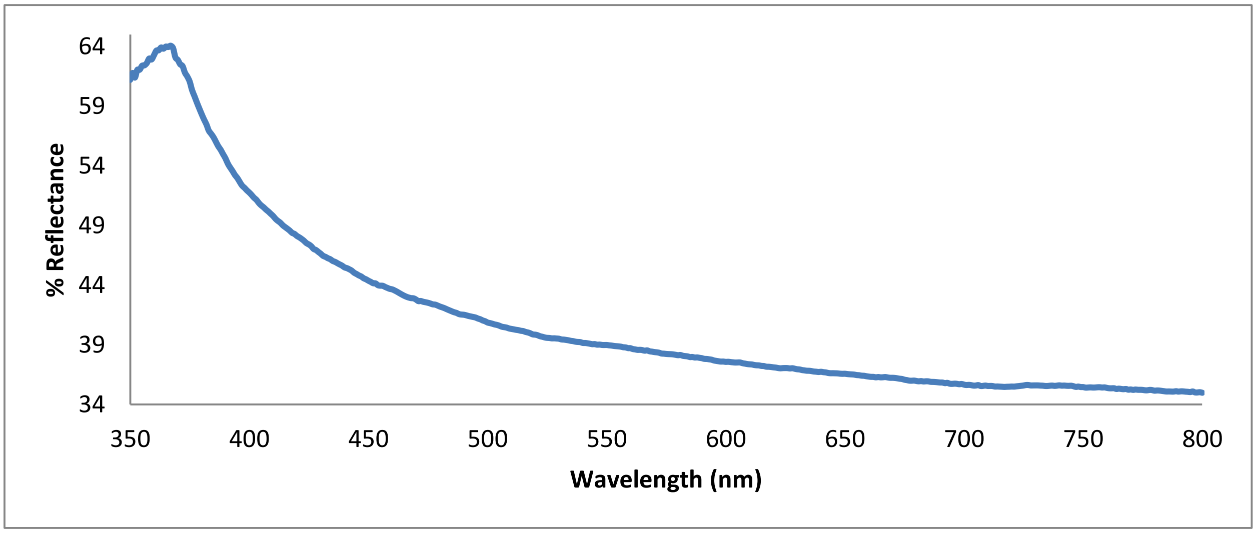

Figure 1: Reflectance on a polished planar silicon

One of the major energy loss mechanisms of solar cells is optical reflection. These losses can be substantially reduced by using AR coatings, which enhance optical absorption on the surface of solar cells.  Optical reflection can be reduced to as low as 6% using an AR coating, compared to 65% for a polished silicon wafer. This is achieved by forming destructive interference of incident light.

However, since its performance is based on a quarter-wavelength coating the lowest reflectivity will only take place at a reduced range of light wavelength and when the incident sunlight is at a particular angle on the surface of the solar cell [19-22]. In their studies, Jung, et. al [23] show that using nanostructures in solar cells may eliminate the need for antireflective coating. They, experimentally, implemented a design using a tradeoff relation between wire length and space-filling ratio where increasing the wire length decreases the wire filling ratio necessary to achieve the same quantity of light absorption. Srivastava, et. al. [24] investigated the reflectivity property of surfaces when a dark black color appeared after removing the silver layer from monocrystalline silicon wafers. Jiansheng, et. al. [25] show that fabrication of one-dimensional (1D) silicon nanostructures supply better device properties than a polished silicon wafer such as efficient charge transport, higher short circuit current and controllable optical properties. Fan et. al. [26] discussed the advantages of enhanced optical absorption due to light trapping by using nanostructures in non-Silicon photoelectric devices. Kayes et. al. [27] provide a device model for the coaxial and radial heterojunctions architecture of this new structure showing improved efficiency over planar devices. There are a number of techniques used for the synthesis of SiNWs [28]. There are two main methods that can be classified as: (i) bottom-up and (ii) top-down. The bottom-up approach involves the addition of material, while the top-down approach generally involves the removal of material from the substrate. A wide variety of nanostructures have been constructed using various techniques [29]. Vapor-liquid-solid (VLS) by chemical vapor deposition (CVD) [30] is a common bottom-up approach. There are other methods such as thermal evaporation [31], molecular beam epitaxy [32], supercritical fluid-liquid-solid [33] and laser ablation [34]. By the other hand, top-down approach uses high quality

single crystal silicon wafers. [35]. There are several methods such as lithography [36], direct reactive ion etching (DRIE) [37] which is an expensive method due to its equipment and materials and the electroless etching method (EE) [38] . The fabrication of nanowires using this method does not require complex sample preparation steps. This technique is effective, having high throughput and low cost. In their studies, Mertens and Sundaram [39] showed that the length of SiNWs, their recession into the planar Si can be controlled by variation of the ratio of HF to $AgNO_3$.

Several authors have reported low reflectance in SiNWs. Among them, Ozdemir, et. al. [40] have reported the preparation of SiNWs by using just one etching solution concentration. Their SiNW arrays of 10 µm achieved a reflectance of 1.3%. Chen el al. reported a reflectance below 5% using the electroless method applying with etching duration more than 2 hours [41]. Huang et al. announced reflectance of 3.1% when the length of the SiNWs arrays is increased to 2.93 µm using the electroless technique [42]. N. Megouda et al [43], has shown decreasing reflectance in the nanostructures down to 1% by applying the same technique and using $HNO_3$ and $NH_4F$ instead of HF. Their results on reflectance are close to the presented in this study. However, adding more precursors to the etching solution may increase the cost of fabrication. A. Smyrnakis et al [44], used e-beam lithography and cryogenic Si plasma etching to grow low reactance SiNWs by controlling the diameter and height of the nanostructures. The results from this process has shown reflectance in SiNWs below 2%. However this process involves equipment and materials which increases the cost of fabrication.

This study shows the optical reflectance in silicon nanowires as a function of the etching solution concentration, etching timings, area of fabrication of the nanostructures and temperature

in the etching solution. Different etching solution concentration were used to grow SiNWs with four different durations of etching of timings. These synthesized structures absorbed up to 98.8 % of incident radiation in the same wavelength range. This result is much better than that of polished planar silicon as they absorbed maximum 65% of the radiation in the same wavelength range analyzed for SiNWs. Also, this result in reflectance is better than achievements accomplished by many authors using the same or different techniques involving more precursors or processes increasing cost of fabrication. The results achieved on decreasing the reflectance in SiNWs presented in this research suggest that these nanostructures could provide a better performance and cost effect results increasing photon absorption and could enhance the carrier collection in solar cells and other optoelectronic devices.

# CHAPTER 3: EXPERIMENTS AND DESIGNS

For all experiments SiNWs arrays were fabricated in a class 1000 clean room at room temperature (23ºC) by silver (Ag) assisted electroless etching method of one side polished single crystal p-type Si (100)-aligned wafers having resistivity of 10 Ω-cm. The Si wafers were cleaned with acetone followed by methanol for 2 minutes each in an ultrasonic bath at room temperature to remove organic deposits from the surface of the substrate. They were rinsed with deionized (DI) water to remove residuals of methanol solution. The substrates were dipped in buffered oxide etch (BOE) for three minutes to remove any surface silicon dioxide grown during the cleaning process and allow the substrate surface to become hydrophobic.

In most of the experiments, the etching process of the cleaned Si wafers was performed at room temperature to obtain vertically aligned SiNWs arrays. For each etching, a single wafer, one square inch in area (2.54 cm on each edge, 6.54 $cm^2$ in area) was used, for each 30 ml of solution. No solution was used twice for an etching.

After etching, each sample was dipped in two baths of 40 ml of DI water for 2 minutes. Subsequently they were dipped in a concentrated nitric acid ($HNO_3$) solution (5 ml of DI water and 20 ml of $HNO_3$) for 25 minutes to completely remove the silver dendrites formed over the SiNWs. They were rinsed in DI water, and dried with a nitrogen ($N_2$) gun.

Hydrofluoric acid is highly hazardous. It causes severe burns that may be not immediately painful or visible. Hydrofluoric acid must be used with safety precautions along with gloves, goggles, eye wash, shower and appropriate containers under a vented fume hood. All the electroless etching experiments were performed under with these safety precautions in

place.

Cross-sectional images of the cleaved SiNWs samples were taken using a HITACHI S-4700 scanning electron microscope (SEM). Digital images of measurements of the SiNWs lengths were acquired and processed by software (QUARTZ PCI) that came with HITACHIS-4700. Reflectance analysis was performed in the visible region (350-800 nm) using a Varian Cary 100 UV-Vis Spectrophotometer.

### 3.1: Investigation on the Reflectance Properties on Silicon Nanowires Grown by Electroless Etching.

Three different etching solutions prepared in a plastic petri dish consisted of silver nitrate ($AgNO_3$) and hydrofluoric acid (HF) diluted in DI water as shown in Table 1. Etching durations used for each of the three concentrations were 15, 30, 45 and 60 minutes.

Table 1: Concentrations of Solutions for 15, 30, 45 and 60 minutes etching time

| Solution | DI $H_2O$ (% Vol., ml) | $AgNO_3$ (% Vol., ml) | HF (% Vol., ml) |
|---|---|---|---|
| 1 | 60, 18 | 23.333, 7 | 16.667, 5 |
| 2 | 60. 18 | 20, 6 | 20, 6 |
| 3 | 60, 18 | 16.667, 5 | 23.333, 7 |

### 3.2: Post cleaning effects on silicon nanowires grown by electroless etching.

Identical etching solutions prepared in plastic petri dishes consisted of 20% (6 ml) 0.1 M silver nitrate ($AgNO_3$) and 20% (6 ml) 49% hydrofluoric acid (HF) diluted in 60% (18 ml) DI water. Subsequently, unstirred samples were prepared by dipping in a solution consisted of 20%

(5 ml) nitric acid ($HNO_3$) and 80% (20 ml) DI water for 25 minutes to remove the silver dendrites formed over the SiNWs. The other set of samples were prepared by the same concentration solution but in a bath that was stirred using a magnetic stirrer at different revolutions per minute (rpm). Stirring cleaning was performed in a multi-position CORNING stirring hot plate model PC-620 at positions 1, 3, 5 and 7. Top view and $45^o$ tilted cross-sectional images of the cleaved SiNWs samples were taken using a scanning electron microscope (SEM).

## 3.3: Area Effect of Reflectance in Silicon Nanowires Grown by Electroless Etching.

Four different area substrates of silicon wafers cut were prepared ranging from 2, 4, 8 and 16 $cm^2$. A concentration of 0.1 M silver nitrate ($AgNO_3$) and 49% hydrofluoric acid (HF) diluted in DI water was used to prepare three different etching solution ratios in plastic petri dishes as presented in Table 2.

Table 2: Concentrations of Etching Solutions for area effect of reflectance in SiNWs

| Solution | DI $H_2O$ (%Vol.,ml) | $AgNO_3$ (%Vol.,ml) | HF (%Vol.,ml) |
|---|---|---|---|
| 1 | 60, 18 | 13.33, 4 | 26.66, 8 |
| 2 | 60. 18 | 16.66, 5 | 23.33, 7 |
| 3 | 60, 18 | 20, 6 | 20, 6 |

## 3.4: Agglomeration in Porous Silicon Prepared From Si-Nanowire Structures

SiNWs are grown using the Electroless etching method. Afterwards, these SiNWs were dipped in a 10 mL anode electrolytic solution concentration containing diluted HF 49% and

$C_2H_6O$ to reduce the quantum confinement of the nanostructures. These electrolytic solution concentration contain 33.33% HF and 66.66% $C_2H_6O$ and etching time during for 15 min at electrical currents of 25 mA and 250 mA. Diagram of this experiment is exhibit in Figure 2 where the SiNWs and a thin lamina of platinum (Pt) were used as anode and cathode respectively.

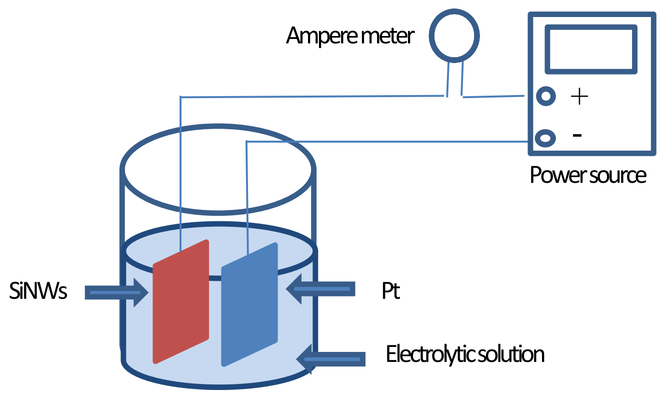


Figure 2: Diagram of the used anode electrolytic etching circuit to reduce the quantum confinement of the SiNWs.

Photoluminescence (excitation/emission) profiles in porous silicon samples were taken using SSE Raman spectra in the Raman spectrometer of the Norfolk University.

3.5: Morphology in Porous Silicon Prepared From Si-Nanowires Grown by Electroless Etching.

Electroless etching technique was used to grow lengthy SiNWs . Then, these SiNWs were dipped in an electrolytic solution containing HF and ethanol ($C_2H_6O$) at a current of 30 mA for 15 min to reduce the diameter and form bunches of nanostructures on the surface. Reflectance and photoluminescence analysis of the prepared nanostructures were performed.

## 3.6: The Effect of Etching Temperature on the Optical Reflectance on Silicon Nanowires Grown by Electroless Etching

The silicon (Si) wafers are dipped for 15 min at different temperatures (25°C, 35°C, 45°C, 55°C) in electroless etching solution prepared in petri dishes containing silver nitrate and hydrofluoric acid. Temperatures in the petri dishes were prepared in a Mary Bath container water in a glass container. The water in the container and the temperature was heated by a COVINE hot plate and controlled by a mercury thermometer.

# CHAPTER 4: RESULT AND DISCUSSION

## 4.1: Investigation on the Reflectance Properties on Silicon Nanowires Grown by Electroless Etching.

This study shows the optical reflectance in silicon nanowires as a function of both etching solution concentration and etching timings. Three different etching solution concentration were used to grow SiNWs with four different durations of etching of timings. These synthesized structures absorbed up to 98.8 % of incident radiation in the same wavelength range. This result is much better than that of polished planar silicon as they absorbed maximum 65% of the radiation in the same wavelength range analyzed for SiNWs. This decrease in reflectance suggests that SiNWs could provide increased photon absorption and could enhance the carrier collection in solar cells and other optoelectronic devices. The cross-sectional SEM pictures of the SiNW arrays prepared by using the three concentrations are shown in Figures 3a-3d, 4a-4d and 5a-5d respectively. It can be seen from these figures that the lengths of the SiNWs change with the HF and $AgNO_3$ concentrations. Digital image acquisition and processing software (QUARTZ PCI) that came with HITACHI S-4700 was used to measure the lengths of the SiNWs.

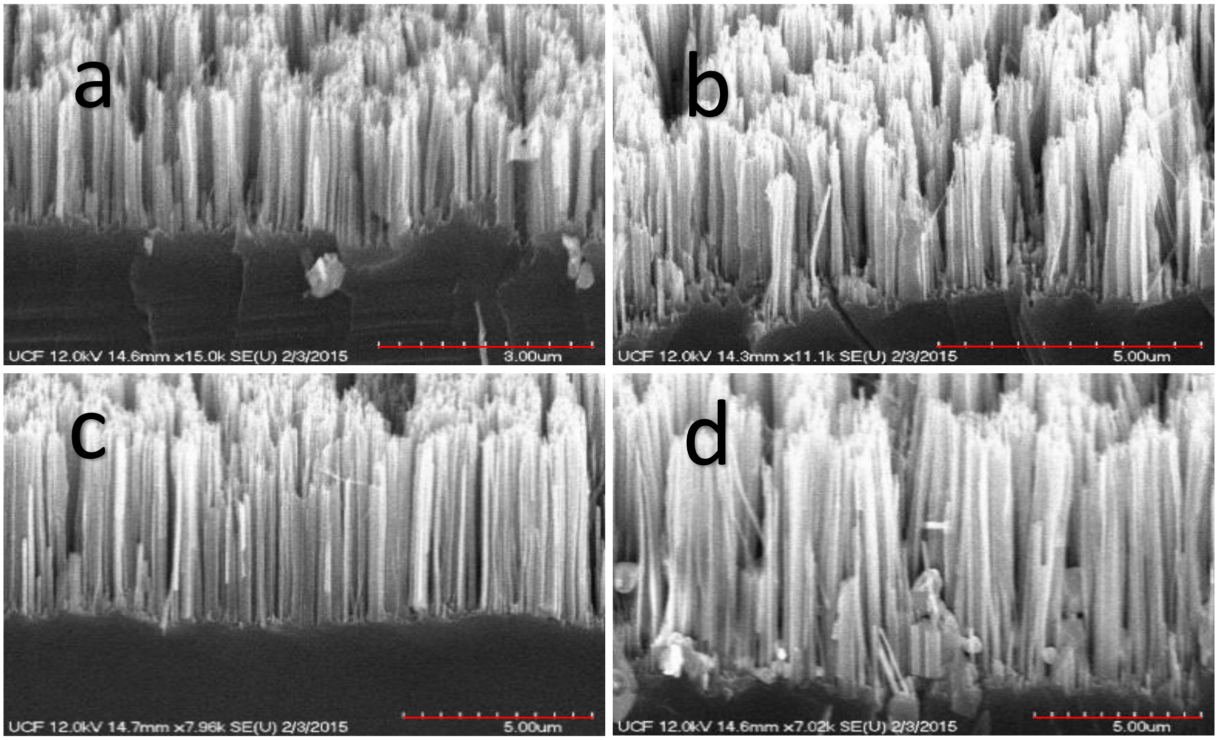

Figure 3: SEM pictures of the SiNWs grown using the concentration of HF 16.66% and $AgNO_3$ 23.33% a) 15 min b) 30 min c) 45 min and d) 60 min.

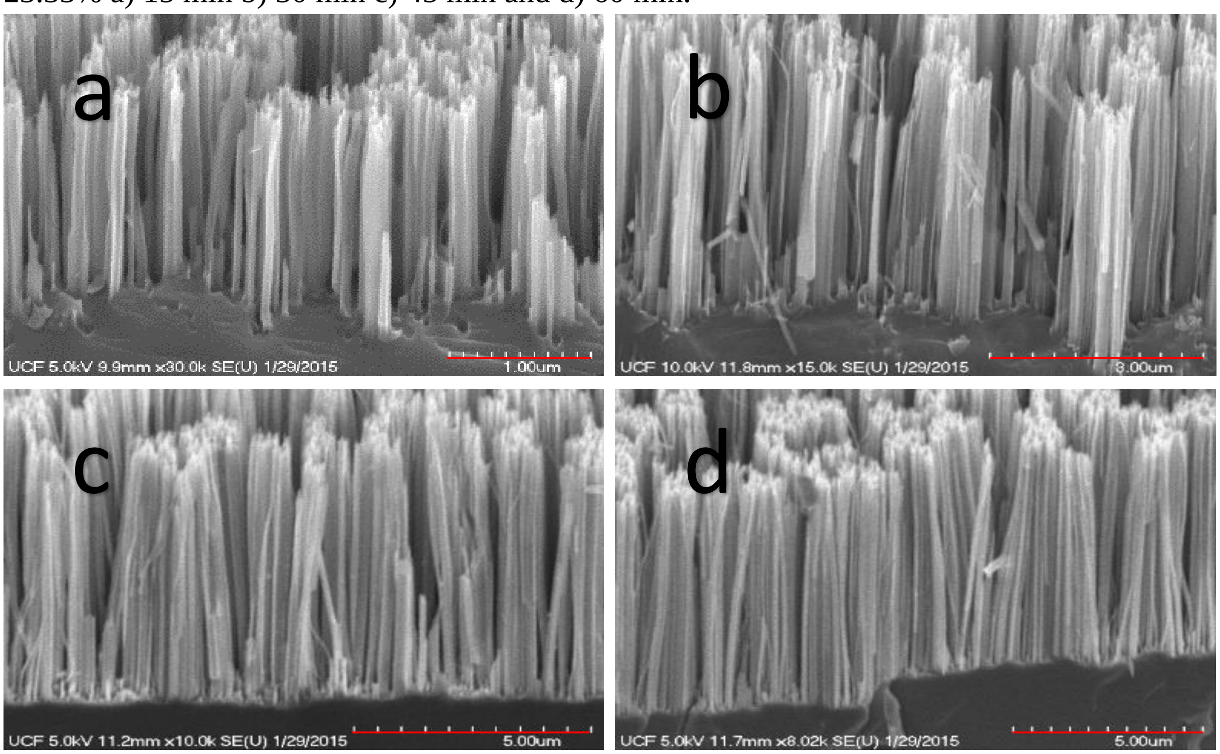

Figure 4: SEM pictures of the SiNWs grown using the concentration of HF 20% and $AgNO_3$ 20% a) 15 min b) 30 min c) 45 min and d) 60 min.

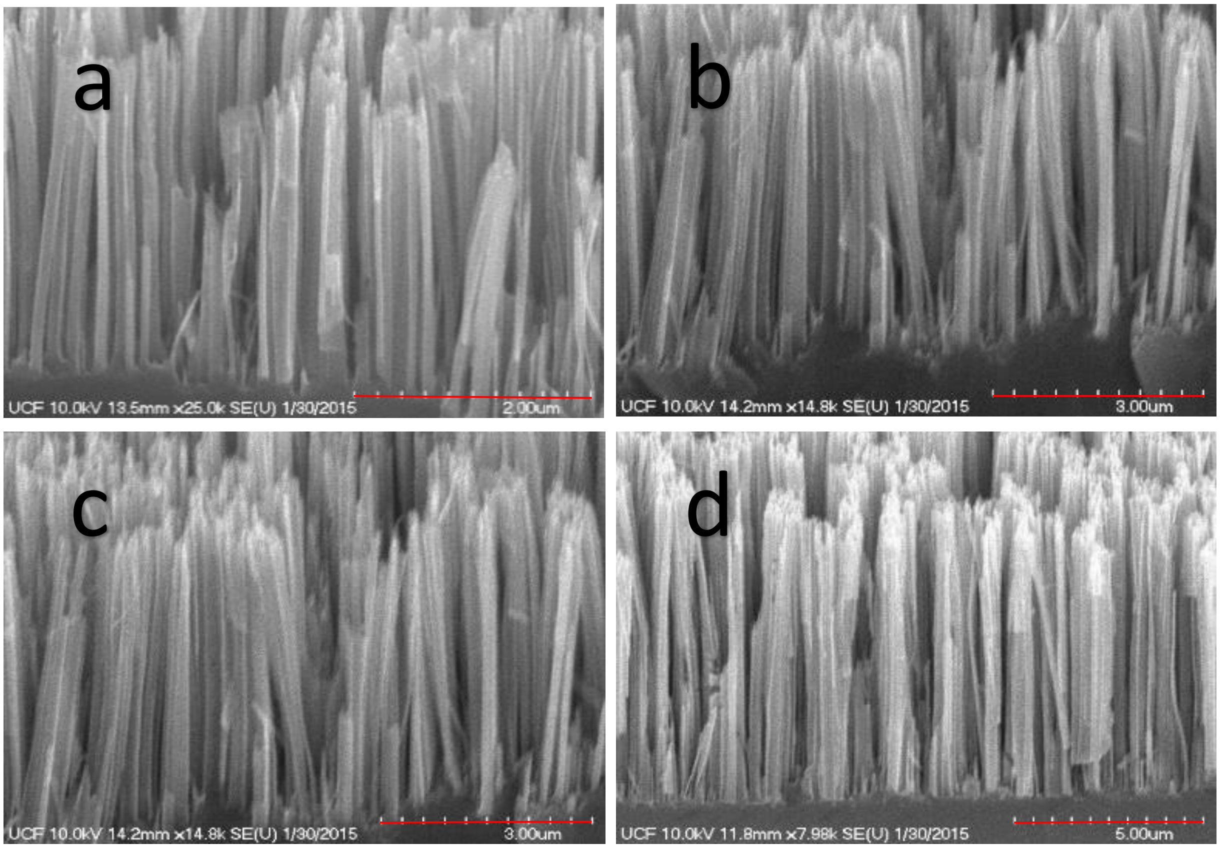

Figure 5: SEM pictures of the SiNWs grown using the concentration of HF 23.33% and $AgNO_3$ 16.66% a) 15 min b) 30 min c) 45 min and d) 60 min.

The etching duration and SiNW array lengths for each concentration is shown in Table 3. Any desired length of the grown SiNWs can be achieved by properly choosing the right concentration and etching time [45].

Table 3: Etching duration and SiNW array lengths for each solution concentration

| Etching time (min) | Solution 1 (µm) | Solution 2 (µm) | Solution 3 (µm) |
|---|---|---|---|
| 15 | 2.195 | 1.739 | 2.680 |
| 30 | 3.161 | 4.193 | 4.292 |
| 45 | 5.794 | 6.186 | 4.399 |
| 60 | 8.735 | 7.043 | 8.035 |

Figure 6 shows the effect of HF and $AgNO_3$ concentrations on the length of SiNW arrays for different etching times. The length of the SiNWs increase with etching time. Taller SiNWs can be achieved with higher concentrations of HF, as seen from the graph. The etching process ceases when any of the precursors is depleted, however, the silver in the solution is depleted most rapidly, since four atoms of silver are used in order to release a single atom of Si [46]. None of the other precursors will run out before this unless the solution is substantially changed. In the reaction of four atoms of silver, six fluorine atoms combine with a single atom of Si, giving these reactions:

$$Ag^{+} + e^{-} \rightarrow Ag \qquad (4.1.1)$$

$$Si + 6F^{-} \rightarrow SiF_6^{2-} + 4e^{-} \qquad (4.1.2)$$

The global reaction is

$$4Ag^{+}(aq) + Si^{0}(s) + 6F^{-}(aq) \rightarrow 4Ag(s) + SiF_6^{2-}(aq) \qquad (4.1.3)$$

Other side reactions with silver are:

$$H_2O \rightarrow H^{+} + OH^{-} \qquad (4.1.4)$$

$$Ag^{+} + OH^{-} \rightarrow AgOH(s) \qquad (4.1.5)$$

and

$$2Ag^{+} + 2OH^{-} \rightarrow Ag_2O(s) + H_2O \qquad (4.1.6)$$

$$2H^{+} + 2e^{-} \rightarrow H_2 \qquad (4.1.7)$$

The depletion rate of silver is dependent on the percentage of HF in the solution and the total area of Si etched.

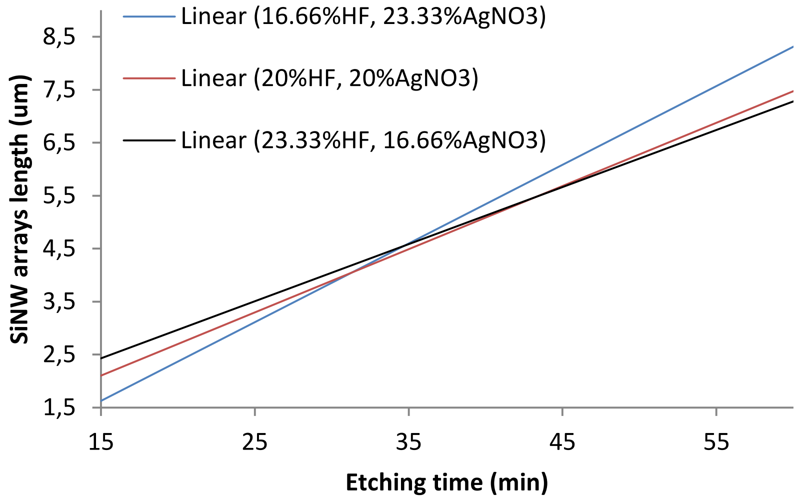


Figure 6: Trend lines of SiNW arrays lengths for solutions 1, 2 and 3 grown at different periods of time; 15 min, 30 min, 45 min and 60 min.

The reflectance studies were performed in the range from 350-850 nm because these wavelengths are the most predominant in the solar spectrum at air-mass (AM) 1.5 [47]. The reflectance plots of the samples are shown in Figures 7(a-c). It can be seen from these figure that when we increase the concentration of HF, the reflectance in SiNWs is lower for wavelengths between 350 and 600 nm. Figures 7b and 7c show that the reflectance is even lower for the same range of wavelengths when we increase the etching time and concentration of HF. However, in Figure 7a it can be seen that the reflectance is higher for the same range of wavelengths when we increase the etching time and have a concentration of $AgNO_3$ 23.33% and a lower concentration of HF 16.66%. This higher reflectance may be due to the agglomeration at the tips of SiNWs. The agglomeration of SiNWs at their tips is mostly attributed to Van der Waals forces [48, 49]. This may be one of the major drawbacks in the fabrication of SiNWs. Wavelength dependence changes with etch time in SiNWs because the longer the etch time, the taller the nanowires, and

the more light they absorb [50].

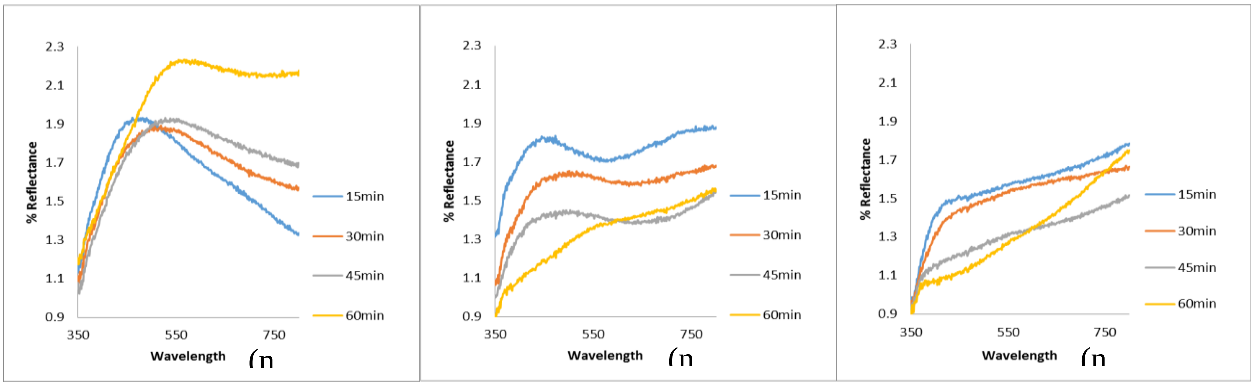


(a) (b) (c)

Figure 7: Reflectance plots as a function of wavelength a) HF 16.66% and $AgNO_3$ 23.33%, b) HF 20% and $AgNO_3$ 20% and c) HF 23.33% and $AgNO_3$ 16.66%.

<u>4.2: Post cleaning effects on silicon nanowires grown by electroless etching.</u>

Low optical reflectance in silicon nanowires (SiNWs) is obtained when a stirring mechanism is introduced during the post-cleaning process. Achieving low optical reflectance may be of great interest for the production of solar cells. These SiNWs were fabricated at room temperature employing the electroless etching technique using an etching solution consisting of silver nitrate and hydrofluoric acid. Experiments show that residual silver dendrites left in the SiNWs array during the electroless etching process may interfere with the reflectance. The results exhibit an optical reflectance in SiNWs as low as 0.7 %.

Reflectance measurements (% R) were obtained across the visible spectrum for the SiNW arrays grown by electroless etching and post cleaned in an unstirred and stirred nitric acid

solution. Also, the reflectance studies on the SiNW arrays cleaned by the stirred mechanism at 60, 300, 550 and 800 rpm are reported in Table 4.

Table 4: Reflectance across the visual spectrum cleaned in unstirred and stirred nitric acid solutions.

| Wavelength (nm) | Unstirred (% R) | Stirred at 800 rpm (% R) | Stirred at 550 rpm (% R) | Stirred at 300 rpm (% R) | Stirred at 60 rpm (% R) |
|---|---|---|---|---|---|
| 350 | 1.2 | 1.5 | 1.1 | 0.8 | 0.7 |
| 600 | 1.7 | 3.3 | 2.3 | 1.5 | 1.2 |
| 800 | 1.8 | 4.6 | 2.9 | 1.6 | 1.6 |

Figures 8a-8b show the 45° cross-sectional and top view SEM pictures of SiNWs cleaned in an unstirred solution of 20% $HNO_3$ and 80% DI water for 25 minutes. It can be seen that silicon structures remained intact after cleaning in an unstirred solutions.

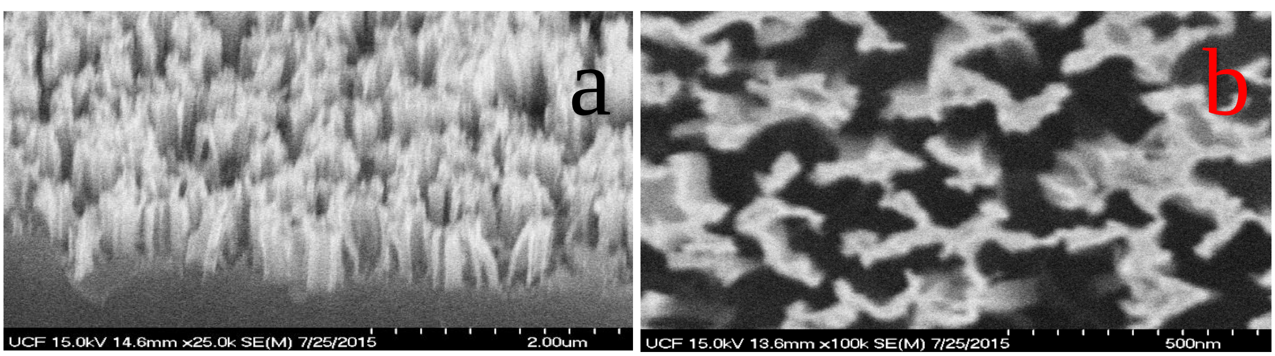

Figure 8: (a) 45° cross-sectional and (b) top view SEM pictures of SiNWs cleaned in an unstirred solution of 20% $HNO_3$ and 80% DI water for 25 minutes.

Different rotational speeds were used to remove silver dendrites from the SiNW arrays during the stirring cleaning process. Figure 9(a-d) and 9(e-h) show the 45° cross-sectional and the top view SEM pictures of SiNWs cleaned under different stirring rates by using the same solution concentration of 20% $HNO_3$ and 80% DI water for 25 minutes respectively. Less number of dendrites are observed when the SiNWs were cleaned in a stirred solution than when

it was done in an unstirred solution. However, broken silicon nanowire nanostructures were observed when the stirring rotational speeds were increased beyond 300 rpm.

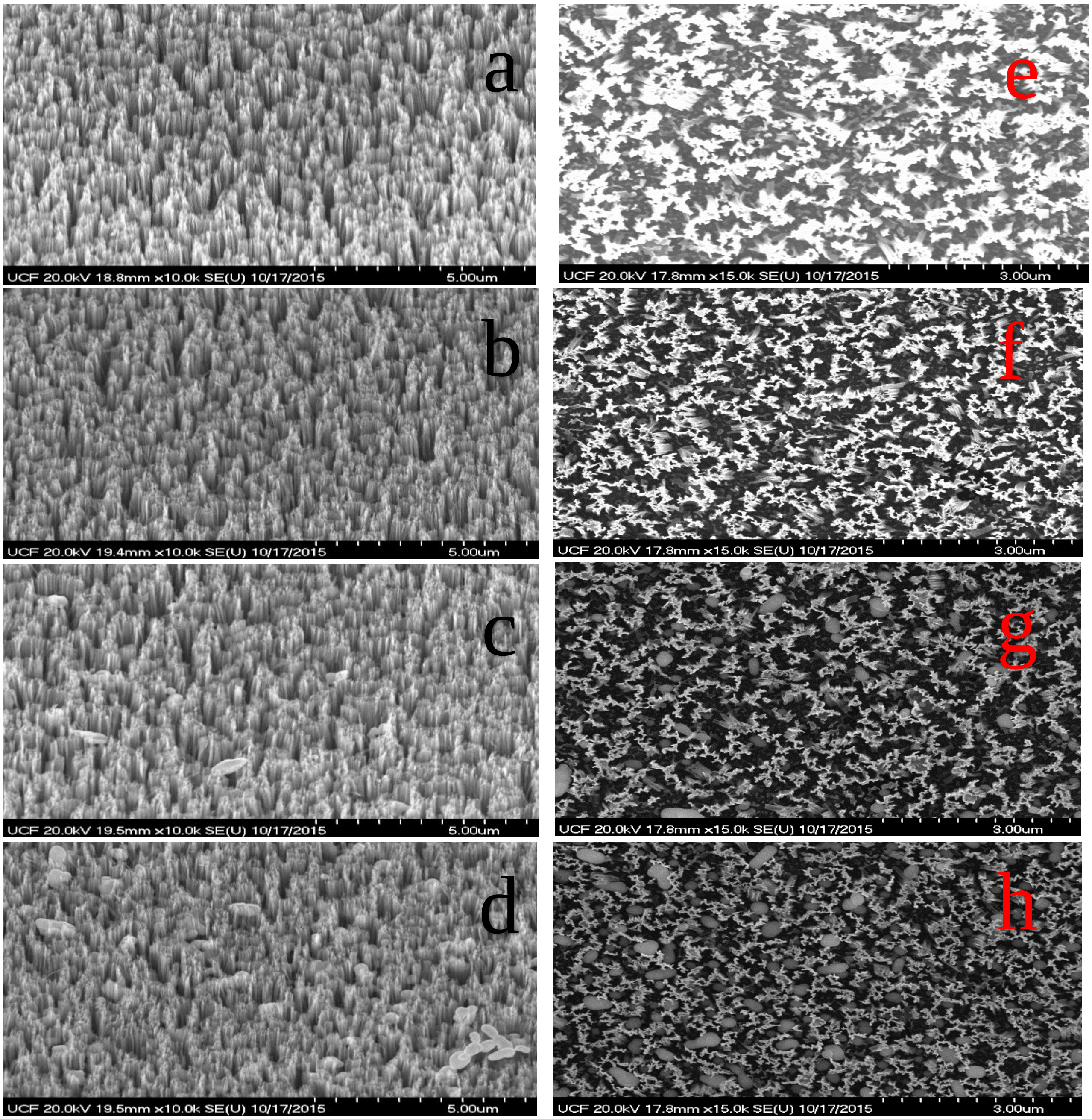


Figure 9: (a-d) 45$^{o}$ tilted cross-sectional and (e-h) top view SEM pictures of SiNWs cleaned in a stirred solution of 20% $HNO_3$ and 80% DI water for 25 minutes at (a, e) 60, (b, f) 300, (c, g) 550 and (d, h) 800 rpm.

Optical reflectance in the 350-800 nm wavelength range was measured for the prepared SiNWs. These wavelengths are the most dominant range in the solar spectrum at air-mass (AM) 1.5. The reflectance plots of the samples are shown in Figure 10. It can be seen that the reflectance in SiNWs was the lowest achieved when the post-cleaning solution was stirred in the range of 60-300 rpm. Whereas, the unstirred SiNWs showed higher reflectance. Post-cleaning performed at lower stirring speeds caused the removal of residual dendrites that were left during the electroless etching process. This in effect caused the decrease of reflectance in the SiNWs. On the other hand, higher stirring speed rates increased the reflectance due to the rupture of the nanostructures.

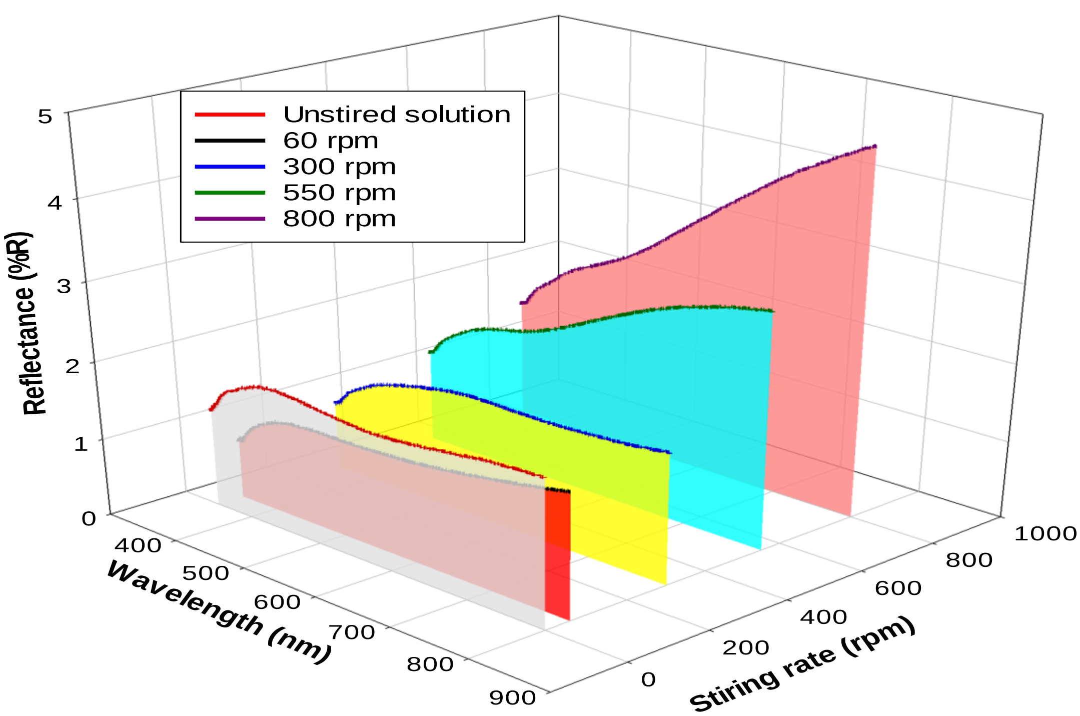


Figure 10: Reflectance plots as a function of wavelength in the visible region for silicon nanowires samples stirred and unstirred in diluted nitric acid solution.

4.3: Area Effect of Reflectance in Silicon Nanowires Grown by Electroless Etching.

This paper shows that the reflectance in silicon nanowires (SiNWs) can be optimized as a function of the area of silicon substrate where the nanostructure growth. SiNWs were fabricated over four different areas of silicon substrates to study the size effects using electroless etching technique. Three different etching solution concentrations of silver nitrate ($AgNO_3$) and hydrofluoric acid (HF) at room temperature were used in the electroless etching process. Experiments show that the reflectance in SiNWs can be decreased when the concentration of silver nitrate is optimized for a determinate size of silicon substrate. The cross-sectional SEM images presented in Figures 11(a)–(d), 12(a)–(d) and 13(a)–(d) respectively shown SiNW arrays prepared by using three concentrations on four different sizes of silicon substrates. It can be seen from these figures that the lengths of the SiNWs change with the concentration of HF and $AgNO_3$ and the size of silicon substrate where the nanostructures are prepared.

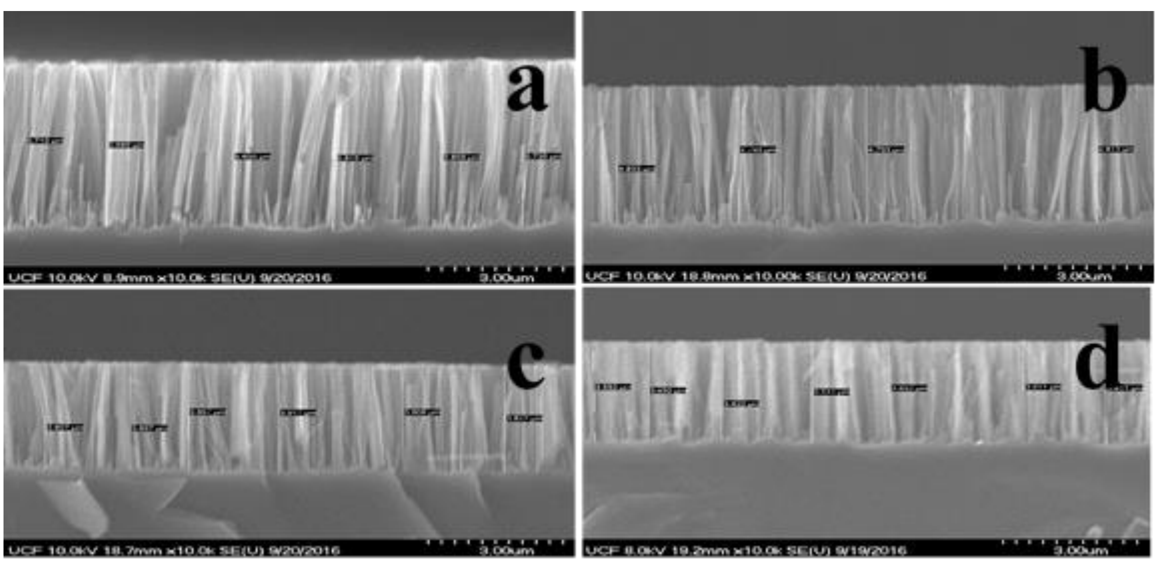


Figure 11: SEM pictures of the SiNWs grown using the concentration of HF 26.666 % and $AgNO_3$ 13.334 % grown in a silicon wafer size surface of (a) 2 $cm^2$ (b) 4 $cm^2$ (c) 8 $cm^2$ and (d) 16 $cm^2$.

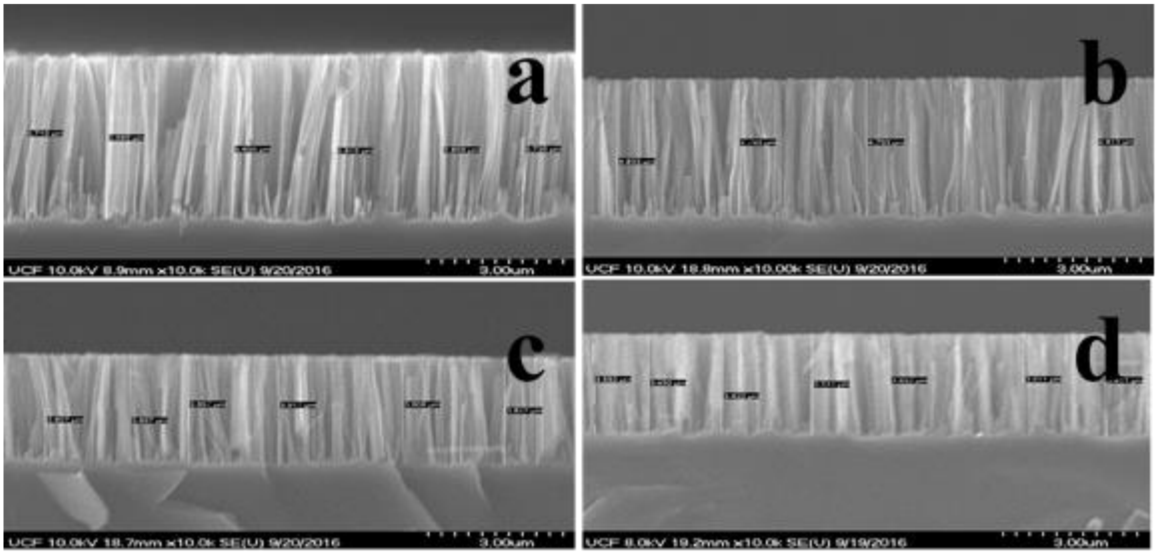


Figure 12: SEM pictures of the SiNWs grown using the concentration of HF 23.33 % and $AgNO_3$ 16.66 % grown in a silicon wafer size surface of (a) 2 $cm^2$ (b) 4 $cm^2$ (c) 8 $cm^2$ and (d) 16 $cm^2$.

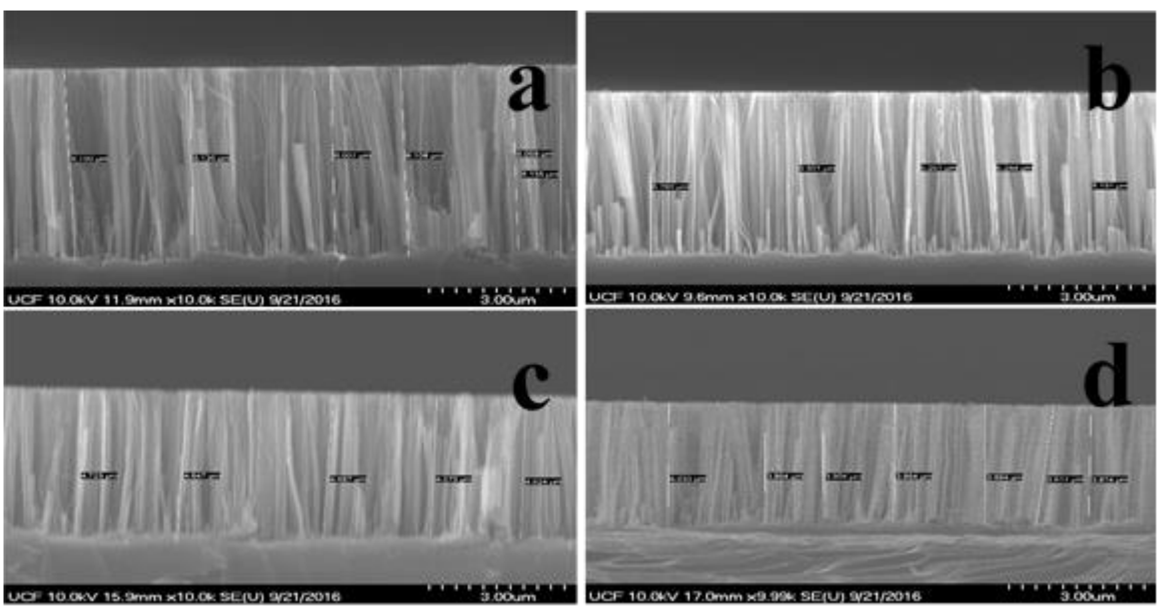


Figure 13: SEM pictures of the SiNWs grown using the concentration of HF 20 % and $AgNO_3$ 20 % grown in a silicon wafer size surface of (a) 2 $cm^2$ (b) 4 $cm^2$ (c) 8 $cm^2$ and (d) 16 $cm^2$.

Figure 14 shows the effect of $AgNO_3$ and HF concentration ratios on the length of SiNW arrays for different wafer surface sizes. The length of the SiNWs increases with the increase in $AgNO_3$ concentration in the etching solution. Taller SiNWs can be achieved with smaller areas of wafer surface. When any of the precursors is depleted the etching process ceases for a determined substrate size, in spite of that, the silver is depleted most rapidly in the solution in larger sizes of silicon substrates, because four atoms of silver are necessary to release a single atom of Si. If the solution or the silicon wafer surface size is substantially changed then one of the other precursors will run out before. In the reaction of four atoms of silver, six fluorine atoms combine with a single atom of Si. It means that as seen in the following reactions:

$$Ag^+ + e^- \rightarrow Ag(s) \tag{4.3.1}$$

$$Si(s) + 2H_2O \rightarrow SiO_2 + 4H^+ + 4e^- \tag{4.3.2}$$

$$SiO_2(s) + 6HF \rightarrow H_2SiF_6 + 2H_2O \tag{4.3.3}$$

In this Si/$AgNO_3$/HF combination occurs a corrosion-redox reaction. Initially, Ag+ ions capture electrons from the valence band of Si reducing the Ag+ ions and oxidizing the silicon where Ag deposits. Ag particles are formed due to this reaction and $SiO_2$ is produced underneath of them. The etching of $SiO_2$ by the HF solution forms vertical shallow pits below the Ag particles resulting in silicon nanowires, as shown in Figure 15.

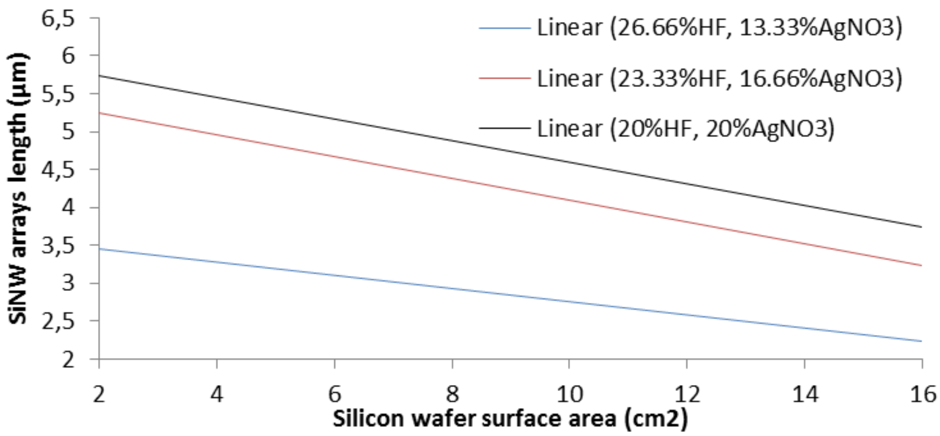


Figure 14: SiNW arrays length as a function of silicon surface areas for different etching solution concentrations.

The dependency of Si NW length falls on etching duration, temperature and solution concentration. However, a detailed and wide range parametric study that enables full control over Si NW length and distribution is missing [51]. Therefore, choosing the right concentration ratio is necessary to achieve lengthy grown SiNWs. Longer and straight nanowires are desired due to the formation of high density and uniform distributed arrays. These features shape a strong light trapping structure in the SiNWs proving lower reflective performance. However, an early depletion of silver in the concentration will decrease the reaction kinetics due to the considerable amount of atoms of Ag necessary to combine with a single atom of Si. This reduction of Ag will lead to cease the sinking mechanism of Ag+ ions towards the bottom of the nanostructures stopping the growth of SiNWs. Therefore, termination of the growing process of SiNWs will affect the light trapping properties of the nanostructures decreasing their antireflection performance. Similarly, an increase of reflectance in SiNWs may be obtained if the area exposed to the electroless etching is increased maintaining the same concentration of the solution due the necessary atoms of Ag for the reaction.

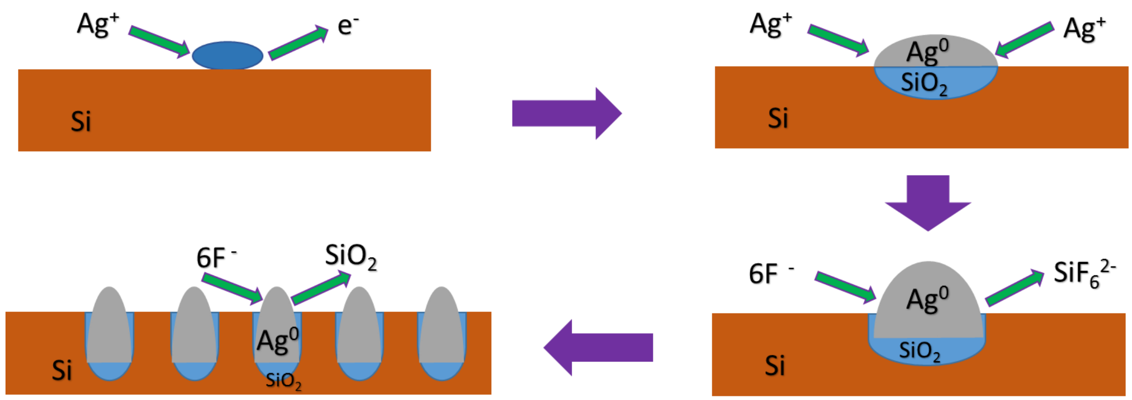


Figure 15: Electroless etching process during SiNWs fabrication.

The percentage of HF in the solution and the total area of Si etched determine the depletion rate of silver. The most predominant wavelengths in the solar spectrum at air-mass 1.5 are in the range from 350–850 nm. The reflectance plots of the samples are shown in Figures 16(a)–(c). It can be seen from these figures that when we increase the concentration of $AgNO_3$ and reduce the wafer surface size, the reflectance in SiNWs is lower for the wavelengths where predominant the solar radiation spectrum.

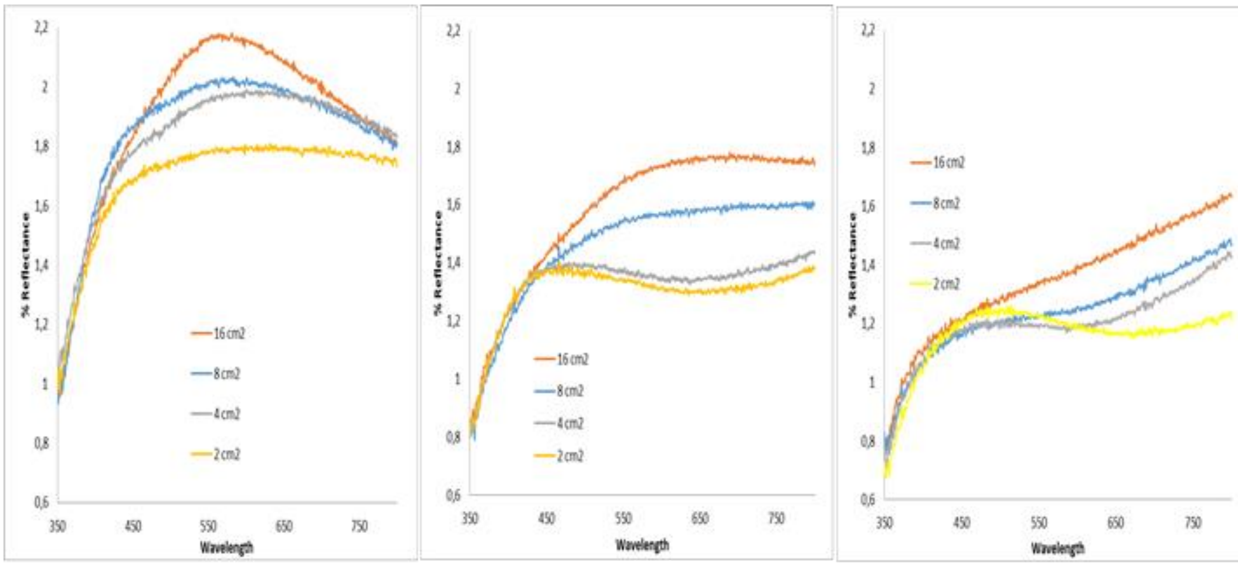


a b c

Figure 16: Reflectance plots of SiNWs prepared with different substrate surface sizes (2, 4, 8 and 16 $cm^2$) for varies concentrations of, (a) HF is 26.66% and $AgNO_3$ is 13.33%, (b) HF is 23.33% and $AgNO_3$ is 16.66% and (c) HF is 20% and $AgNO_3$ is 20%.

4.4: Agglomeration in Porous Silicon Prepared From Si-Nanowire Structures

Porous silicon nanowires have showed several advantages including low reflection and high luminescence characteristics for the range of the optical spectrum. This indicates that porous SiNWs have a great potential to be utilized in optoelectronics and chemical sensors. In this document silicon nanowires have been grown at room temperature for 30 minutes using the electroless etching method at determinate etching concentration of silver nitrate and hydrofluoric acid based solution. Porous SiNWs have been fabricated from electroless SiNWs in an electrolytic process in different ethanol and hydrofluoric acid based solutions concentration, electrical current and etching times. Analysis determining relationship between optical diffuse

reflectance and photoluminescence is presented.

Nanostructures present different changes due to their small diameter. The increase of the apparent elastic modulus of SiNWs is one of the changes and is attributed to surface tension due to the increase of the electrical current during the etching process [52]. Surface tension produces a residual stress field in the bulk of nanowires deforming the nanostructures and creating bunching at the surface but increasing the intensity of luminescence in SiNWs. Results in photoluminescence when the electrical current is increased is reported in Figures. 3a and 3b. In these 3D top views of photoluminescence red represents the most intense features while blue and magenta represent the least intense feature when the porous SiNWs are exposed to an ultraviolet lamp. There is particular interest is the emission maximum at 290:685 (excitation: emission) in Figure 17a, but it doesn't shows a high intensity in luminescence as seen in peaks at 625 and 685nm in Figure 17b.

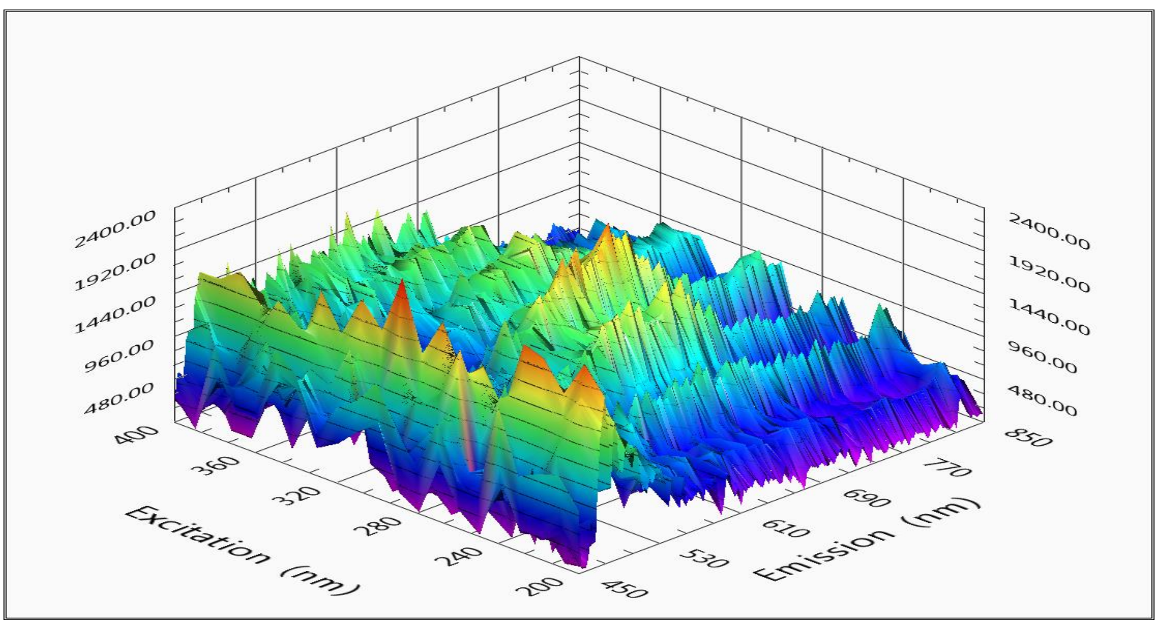

(a)

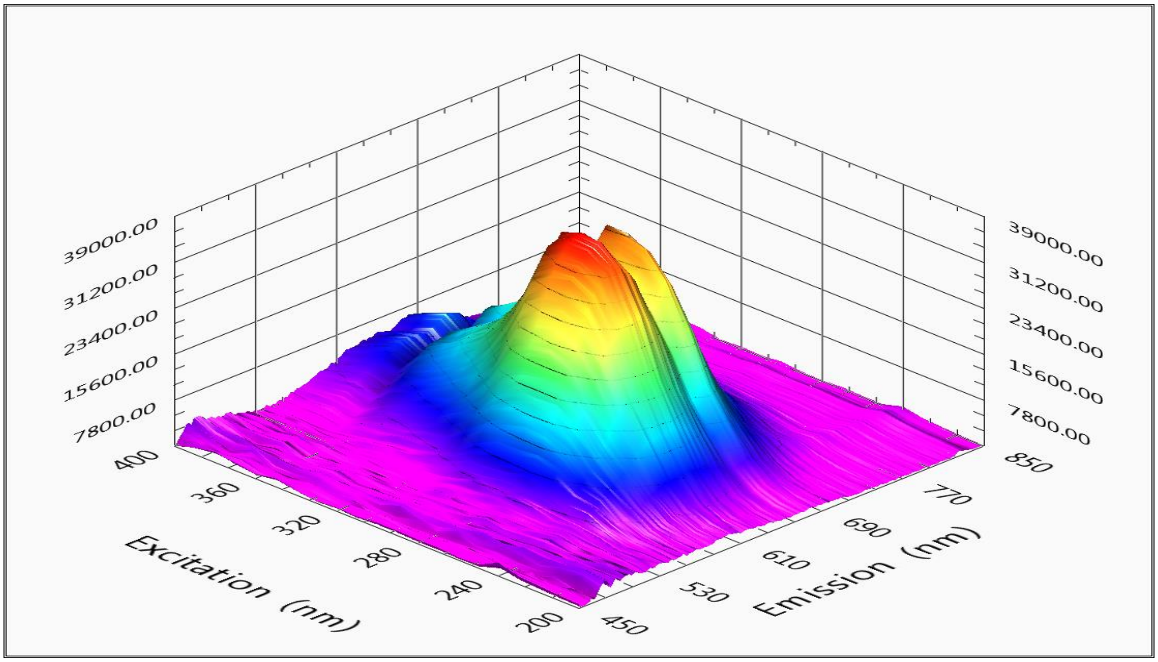


(b)

Figure 17: 3D photoluminescence spectrum when ultraviolet light is exposed on porous SiNWs fabricated in a solution concentration containing a) 33.33% HF and 66.66% $C_2H_6O$ for 15 min etching time at 25 mA, and b) 33.33% HF and 66.66% $C_2H_6O$ for 15 min etching time at 250 mA.

Additionally, reflectance measurements (% R) were obtained across the visible spectrum in SiNWs and porous SiNWs. Porous SiNWs were fabricated in an anode electrolytic solution concentration containing 33.33% HF and 66.66% $C_2H_6O$ for 15 min etching time at 25 mA, and 33.33% HF and 66.66% $C_2H_6O$ for 15 min etching time at 250 mA. Enhanced optical absorption in porous SiNWs may be achieved at lower electrical currents. Even better absorption of the optical light in nanostructures is shown when SiNWs are grown using the electroless technique. Traces of percentage of diffuse optical reflectance in silicon structures in

the visible region 350-800 nm is shown in Figure 18 and measurements are reported in Table 5.

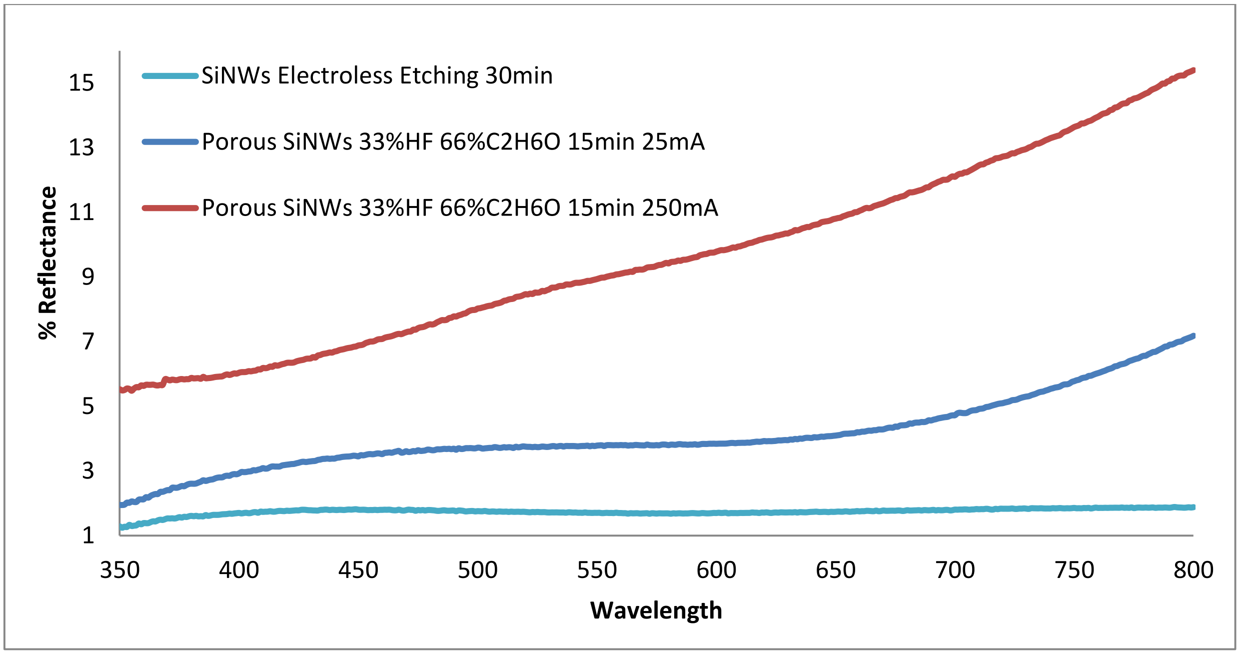


Figure 18: Reflectance analysis across the visible spectrum of SiNWs grown using the electroless technique and porous SiNWs fabricated from prepared electroless SiNWs.

Table 5: Reflectance across the visual spectrum in SiNWs grown using the electroless technique and porous SiNWs fabricated from prepared electroless SiNWs.

| Wavelength (nm) | Electroless Technique SiNWs (%R) | Porous SiNWs 25 (mA) (%R) | Porous SiNWs 250 (mA) (%R) |
|---|---|---|---|
| 350 | 1,2 | 1,9 | 5,5 |
| 600 | 1,7 | 3,8 | 9,8 |
| 800 | 1,8 | 7,2 | 15,4 |

4.5: Morphology in Porous Silicon Prepared From Si-Nanowires Grown by Electroless Etching.

Porous silicon nanowires have shown several advantages including low reflection and high luminescence characteristics for the range of the optical spectrum. This indicates that porous

silicon nanowires have a great potential to be utilized in optoelectronics and chemical sensors. In this document, silicon nanowires (SiNWs) are grown using the electroless etching technique at specific etching time and concentration of silver nitrate and hydrofluoric acid based solution. Subsequently, porous SiNWs are fabricated from the electroless etched SiNWs in an electrolytic process in ethanol and hydrofluoric acid based solutions keeping the same electrical current and etching time. Analysis determining the relationship between reflectance and length and diameter of the nanostructures is presented.

Cross-section porous silicon nanowire SEM image is shown in Figure 19. This rough appearance may be due to the removal of oxidized silicon when the prepared nanostructures are etched in the electrolytic etching solution containing HF and $C_2H_6O$ leading to the formation of porous SiNWs. Further etching may occur at the pore sidewalls when $C_2H_6O$ is increased reducing the diameter and length of the nanostructures, as shown in cross-section SEM images in Figure 20. SiNW array lengths and diameters for each solution are shown in Table 6.

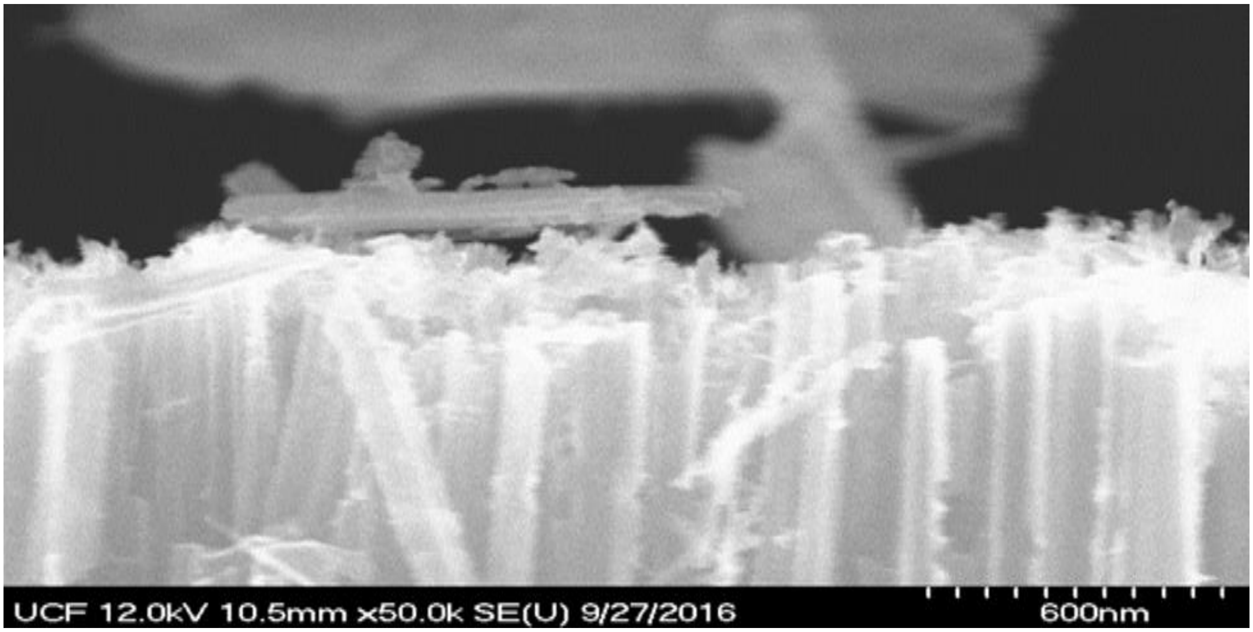


Figure 19: Cross-section SEM image showing the top part of porous silicon nanowires structures when prepared SiNW arrays are etched in an electrolytic solution at room temperature, and an electric current of 30mA for 15 minutes.

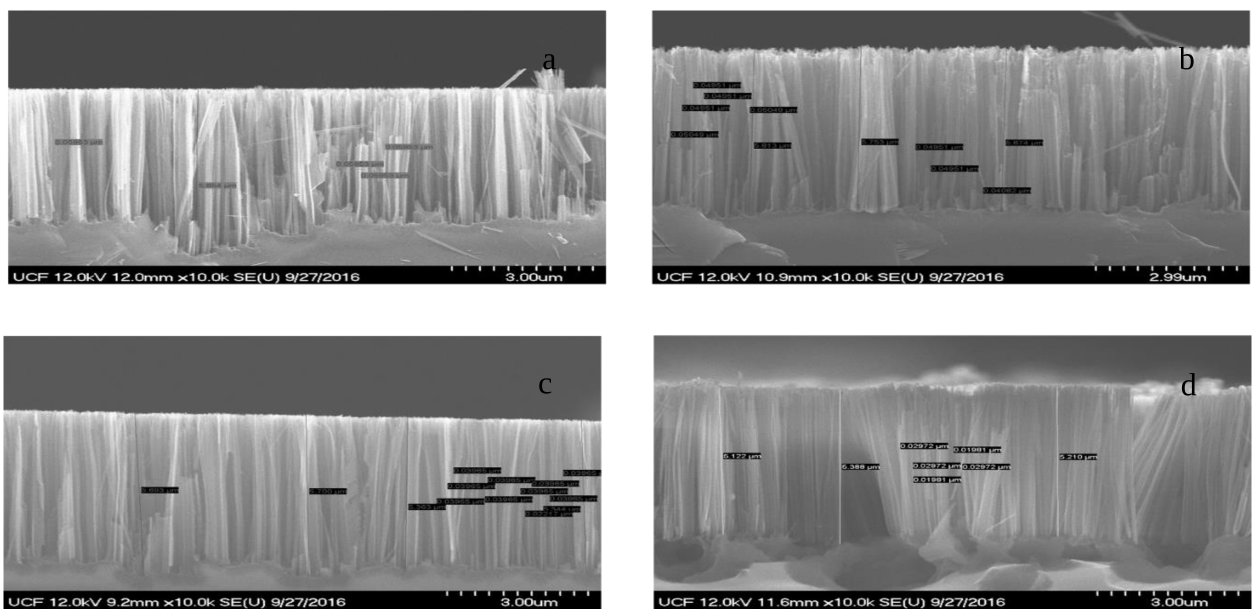


Figure 20 temperature: Cross-section SEM imagens of porous SiNWs prepared in an electrolytic solution at room and with a current of 30mA for 15 minutes containing a) 80% HF and 20% $C_2H_6O$, b) 60% HF and 40% $C_2H_6O$, c) 40% HF and 60% $C_2H_6O$ and d) 20% HF and 80% $C_2H_6O$.

Table 6: Lengths and diameters of SiNW and porous SiNW arrays grown using different solutions.

| Process | Electroless | Porous SiNWs prepared in: | | | |
|---|---|---|---|---|---|
| Dimension | 20%HF and 20% $AgNO_3$ | Solution 1 | Solution 2 | Solution 3 | Solution 4 |
| Length (um) | 6.11 | 5.85 | 5.75 | 5.65 | 5.38 |
| Diameter (um) | 0.07 | 0.06 | 0.05 | 0.04 | 0.03 |

These changes in the morphology of silicon nanostructures may be attributed to the solution concentration. Increasing concentration of $C_2H_6O$ can readily diffuse away from the etching front to lattice defects on the surface of the already formed SiNWs. This may result in formation of porous SiNWs and may cause ruptures at the top of the nanostructures. Increasing of reflectance in porous SiNWs is seen from 550-800 nm when concentration of $C_2H_6O$ is increased. Diffuse optical reflectance in silicon structures in the visible region 350 nm-800 nm are shown in Figure 21.

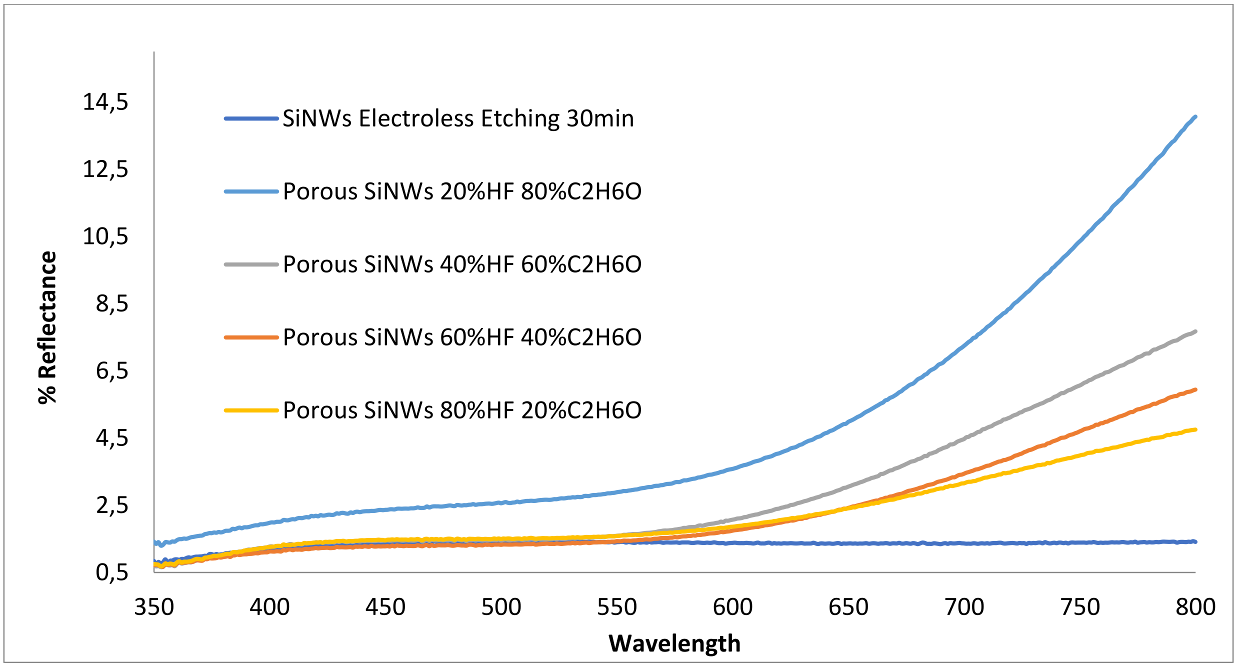

Figure 21: Reflectance analysis in SiNWs and porous SiNWs across the visible spectrum.

4.6: The Effect of Etching Temperature on the Optical Reflectance on Silicon Nanowires Grown by Electroless Etching.

In this document, silicon nanowires have been fabricated at different temperatures by electroless etching method using silver nitrate and hydrofluoric acid based solution. Analysis determining relationships between optical diffuse reflectance in silicon nanowires and different temperatures are presented.

Traces of percentage of diffuse reflectance in SiNWs as a function of optical region (350-800nm) are presented in Figure 22. It shows high reflectance in the samples when the temperature is increased. These samples were fabricated in a solution bath with concentration of 20% HF, 20% $AgNO_3$, and 60% DI $H_2O$ at temperatures of 25$^oC$, 35$^oC$, 45$^oC$ and 55$^oC$ for 15 minutes of etching time. Different lengths of SiNW arrays, shown in Table 7 and Figure 23, are obtained when the nanostructures are grown at different temperatures at the same etching concentration during 15 minutes. Enhanced optical reflectance may be achieved at lower etching solution temperatures. Low temperature slows the kinetics reaction that will allow to grow uniform and well aligned SINWs (Fig. 24a) contrary to randomly directed nanowires growth at high temperatures (Fig. 24b). Further increase in the temperature in the electroless etching solution during the SiNWs fabrication revealed a higher reflectance for the samples. Conducting electroless etching at high temperatures cause the increase in agglomeration of the nanowires (Fig. 24c and 24d). A uniform growth of SiNWs could optimize nanowire spacing that would improve charge collection and enhance optical reflectance.

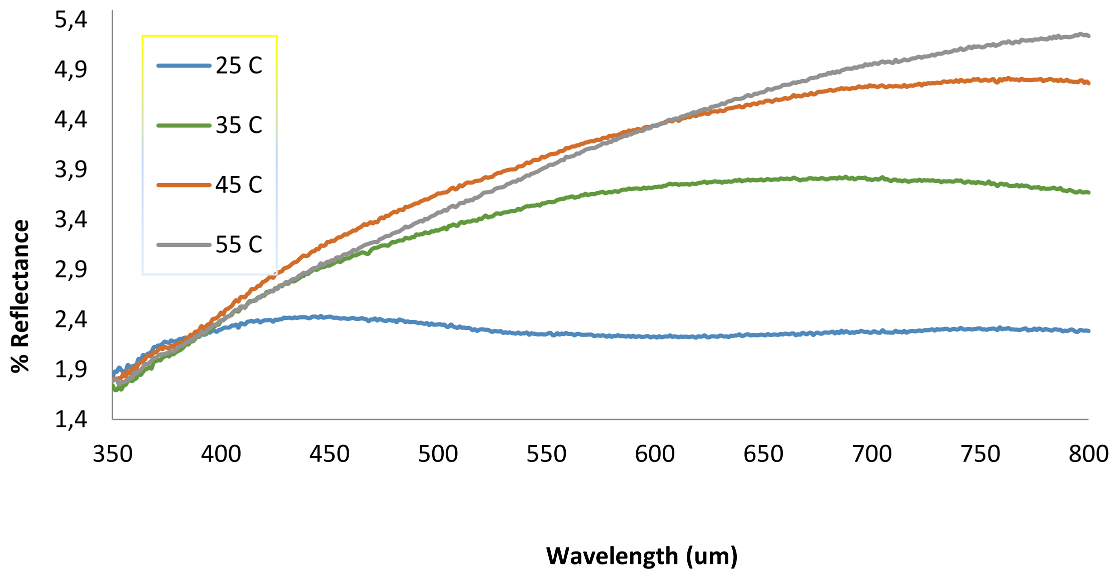


Figure 22: Reflectance analysis across the visible spectrum of SiNWs grown by electroless etching at different temperatures during 15 minutes in a solution bath with concentration of 20% HF, 20% $AgNO_3$, and 60% DI $H_2O$.

Table 7: SiNWs arrays lengths measured at different temperatures

| Etching Temperature (ºC) | Length of SiNWs (µm) |
|---|---|
| 25 | 1,3 |
| 35 | 2,8 |
| 45 | 3,5 |
| 55 | 4,2 |

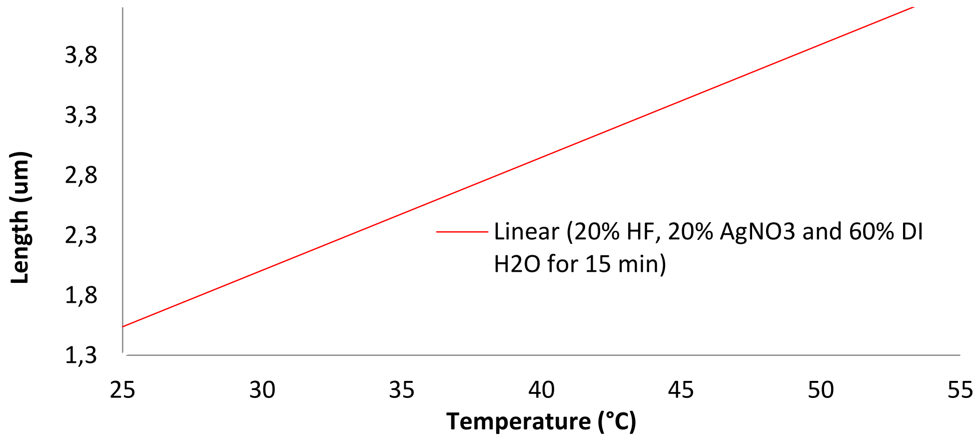


Figure 23: Trend lines of SiNW arrays lengths grown by electroless etching at temperatures of 25°C, 35°C, 45°C, 55°C during 15 minutes in a solution bath with concentration of 20% HF, 20% $AgNO_3$, and 60% DI $H_2O$.

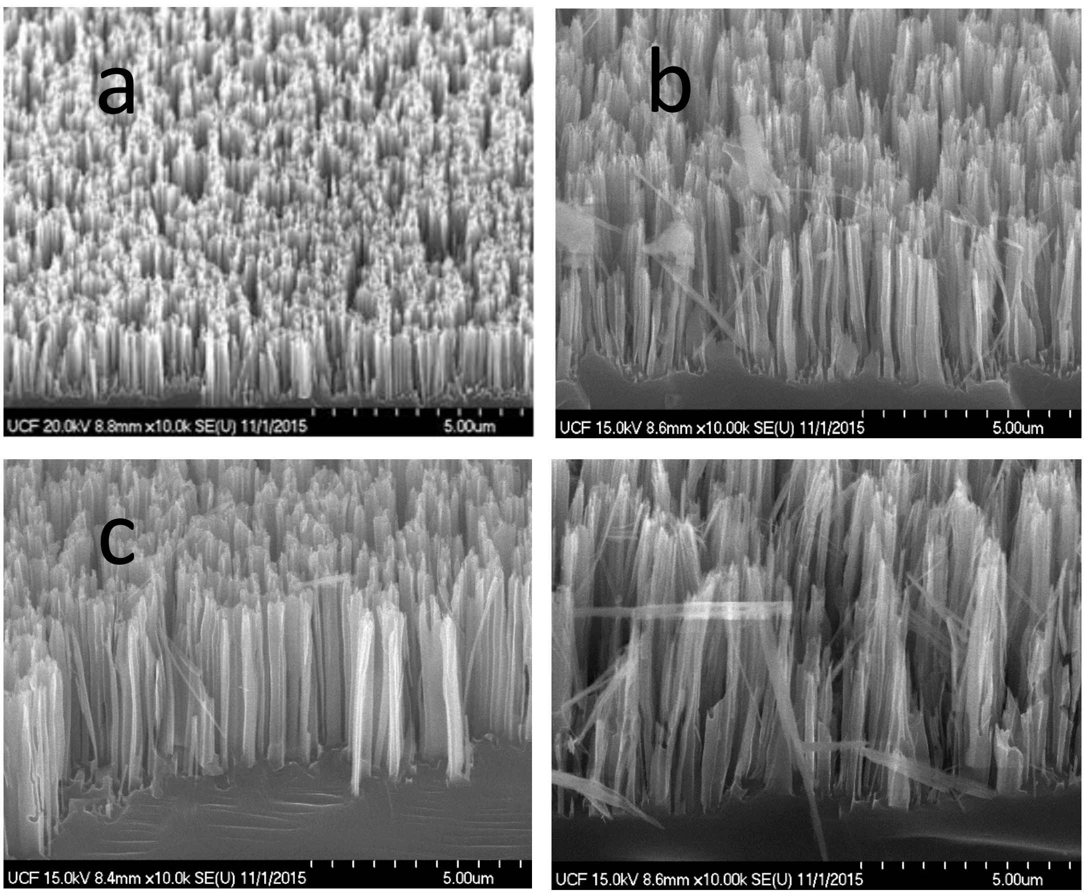


Figure 24: Cross sectional SEM images of SiNW arrays obtained by electroless etching during 15 minutes conducted at (a) 25°C (b) 35°C (c) 45°C (d) 55°C.

# CONCLUSIONS

Highly oriented silicon nanowires prepared by electroless etching method can significantly suppress light reflection across a broad spectrum. Higher concentrations of HF in the electroless etching solution produced lower reflectance in the samples. A lower reflectance in SiNWs is achieved when the etching time is higher.  An optimum concentration of HF is 20% and of $AgNO_3$ is 20% in the etching solution that produces the best absorption in SiNWs. This concentration also has an optimum absorption when the etching time is closer to one hour. In order to achieve lower reflectance properties for SiNW arrays the balance of concentration of HF and $AgNO_3$ solution is required.

Electroless grown nanostructures were cleaned by a stirring process and compared with an un-stirred process to remove the silver dendrites and residues in the SiNW arrays for a specific length of time. The cleaned and synthesized structures using a stirred mechanism absorbed up to 99.30 % and 98.8 % of incident radiation at 350 nm and between 351 nm 650 nm optical wavelength ranges respectively. This result is much better than the absorption seen for the unstirred post cleaning method in the same wavelength range. This decrease in optical reflectance suggests that SiNWs could provide increased photon absorption and could enhance the carrier collection in solar cells and other optoelectronic devices. This is due to the removal of silver dendrites at lower speed stirred solutions.

SiNWs prepared by electroless etching method can significantly increase light absorption abroad the solar light spectrum. Lower reflectance in the samples is produced when $AgNO_3$ is increased in the etching solution. A lower reflectance in SiNWs is achieved when the silicon substrate size is reduced. However, an optimum concentration of 20% HF and 20% $AgNO_3$ in

the etching solution produces the best absorption in SiNWs for the smaller area studied in this experiment, 2 $cm^2$, and wavelengths greater than 600nm. In order to achieve lower reflectance performance in SiNW arrays, solution concentrations of HF and $AgNO_3$ and the size of the samples must be controlled during the SiNWs growth.

Quantum confinement effect and surface defects affect the photoluminescence in porous silicon nanowires. Significant photoluminescence may be achieved when electrical current is increased during the fabrication of porous SiNWs. However, optical reflectance in the nanostructures may increase due the ununiformed manner how the porous SiNWs are grown causing inefficient charge collection.

Porous silicon nanowires prepared in a lower concentration of HF and higher concentration of $C_2H_6O$ may remove oxide on the prepared SiNWs due to the lower holes consumption rate. These variation in solution concentration may affect the morphology of the porous silicon nanowires structure re ducing the length and diameter. However, optical reflectance in the nanostructures may increase due non-uniform porous SiNWs structures causing inefficient charge collection.

Increasing the temperature in the electroless etching solution during the SiNWs fabrication may cause nanowires to get stuck to each other. It may affect the collection of carrier process increasing the optical reflectance performance of the samples. A uniform growing of SiNWs could optimize nanowire spacing that would improve charge collection and enhance optical reflectance.

# REFERENCES


[1] D. Zschech, D. H. Kim, A. P. Milenin, R. Scholz, R. Hillebrand, C. J. Hawker, T. P. Russell, M. Steinhart, U. Go¨sele, Nano Lett. 2007, 7, 1516.

[2] Y. Zhu, G. S. Cheng, L. D. Zhang, J. Mater. Sci. Lett. 1998, 17, 1897.

[3] Treuting, R. G.; Arnold, S. M. Acta Met. 1957, 5, 598.

[4] A. M. Morales, C. M. Lieber, Science 1998, 279, 208.

[5] X.Y. Zhao, C.M. Wei, L. Yang, M.Y. Chou, Quantum confinement and electronic properties of silicon nanowires. Phys Rev. Lett. 92, 236805 (2004)

[6] D.Y. Li, Y.Y. Wu, P. Kim, L. Shi, P.D. Yang, Thermal conductivity of individual silicon nanowires. Appl Phys. Lett. 83, 2934 (2003)

[7] Y. Cui, C.M. Lieber, Functional electronic devices assembled using silicon nanowire building blocks. Science 291, 851 (2001)

[8] Schmidt V, Riel H, Senz S, Karg S, Riess W and Gosele U 2005 Realization of a silicon nanowire vertical surroundgate field effect transistor Small 2 85–8

[9] Goldberger J, HochbaumA I, Fan R and Yang P 2006 Silicon vertically integrated nanowire field effect transistors Nano Lett. 6 973–7

[10] Hochbaum A I, Chen R K, Delgado R D, Liang W J, Garnett E C, Najarian M, Majumdar A and Yang P D 2008 Enhancedthermoelectric performanceof rough silicon nanowires Nature 451 163–7

[11] Boukai A I, Bunimovich Y, Tahir-Kheli J, Yu J K, Goddard W A and Heath J R 2008 Silicon nanowires as efficient thermoelectric materials Nature 451 168

[12] Cui Y, Wei Q, Park H and Lieber C M 2001 Nanowire nano-sensors for highly sensitive and selective detection of biological and chemical species Science 293 1289–92

[13] Bae J, Kim H, Zhang X M, Dang C H, Zhang Y, Choi Y J, Nurmikko A and Wang Z L 2010 Si nanowire metal–insulator–semiconductor photodetectors as efficient light harvesters Nanotechnology 21 095502

[14] Chan C K, Patel R N, O’Connell M J, Korgel B and Cui Y 2010 Solution-grown silicon nanowires for lithium-ion battery anodes ACS Nano 4 1443–50

[15] Chan C K, Peng H, Liu G A O, Zhang X F, Huggins R A and Cui Y I 2008 High-performance lithium battery anodes using silicon nanowires Nat. Nanotechnol.3 31–5

[16] Qian F, GradecakS, Li Y, Wen C Y and Lieber C M 2005 Core multi shell nanowire hetero structures as multicolor high efficiency light emitting diodes Nano Lett. 5 11

[17] Hu L and Chen G 2007 Analysis of optical absorption in silicon nanowire arrays for photovoltaic applications Nano Lett. 7 3249–52

[18] Sivakov V, Andr¨a G, Gawlik A, Berger A, Plentz J, Falk F and Christiansen S H 2009 Silicon nanowire-basedsolar cells on glass: synthesis, optical properties, and cell parametersNano Lett. 9 1549

[19] S. Walheim, E. Schaffer, J. Mlynek and U. Steiner, Science. 283 (1999) 520–522.

[20] M. L. Kuo, D. J. Poxson, Y. S. Kim, F. W. Mont, L. K. Kim, E. F. Schuhert and S. Y. Lin, Opt. Lett. 33 (2008) 2527–2529.

[21] S.-S. Lo, C.-C. Chen, F. Garwe and T. Pertch, J. Appl. Phys. 40 (2007) 754–758, DOI:10.1088/0022-3727/40/3/010.

[22] L. L. Ma, Y. C. Zhou, N. Jiang, X. Lu, J. Shao, W. Lu, J. Ge, X. M. Ding and X. Y. Hou, Appl. Phys. Lett. 88 (2006) 171907.

[23] Jin-Young Jung, Han-Don Um, Sang-Won Jee, Kwang-Tae Park, Jin Ho Bang, Jung-Ho Lee, Optimal design for antireflective Si nanowire solar cells, Solar Energy Materials & Solar Cells. 112 (2013) 84-90.

[24] Srivastava S K, Kumar D, Singh P.K, Kar M, Kumar V and Husain M., Excellent antireflection properties of vertical silicon nanowire arrays, Sol. Energy Mater. Sol. Cells 94 (2010) 1506-1511.

[25] Jiansheng J, Zhang W, Peng K.Q, Yuan G, Lee C S and Lee S T., Surface-dominated transport properties of silicon nanowires, Adv. Funct. Mater. 18 (2008) 3251–3257.

[26] Fan Z, Ruebusch D J, Rathore A.A., Kapadia R, Ergen O, Leu P.W. and Javey A., Challenges and prospects of nanopillar based solar cells, Nano Res. 2 (2009) 829–843.

[27] Kayes B.M., Atwater H.A. and Lewis N.S., Comparison of the device physics principles of planar and radial p–n junction nanorod solar cells, J. Appl. Phys. 97 (2005) 114302

[28] C.M. Lieber, Solid State Commun. 107 (1998) 607.

[29] Y.N. Xia, P.D. Yang, Y.G. Sun, Y. Wu, N. Mayers, B. Gates, Y. Yin, F. Kim, and H. Yan, Adv. Mater. 15 (2003) 353.

[30] R.S. Wagner and W.C. Ellis, Appl. Phys. Lett. 4 (1964) 89.

[31] Yu D.P., Nanoscale silicon wires synthesized using simple physical evaporation Appl. Phys. Lett. 72 (1998) 3458.

[32] Buttner C.C, Zakharov N.D, Pippel E, Gosele U. and Werner P., Gold-enhanced oxidation of MBE-grown silicon nanowires Semicond., Sci. Technol. 23 (2008) 75040.

[33] Holmes J.D, Johnston K.P., Doty R.C. and Korgel B.A., Science 287 (2000) 1471.

[34] Morales A.M. and Lieber C.M., A laser ablation method for the synthesis of crystalline semiconductor nanowires, Science 279 (1998) 208–211.

[35] R. Juhasz, K. Kylm€anen, A. Galeckas, and J. Linnros, Mater. Sci. Eng. 25 (2005) 733.

[36] Mart J. and Garcia R., Silicon nanowire circuits fabricated by AFM oxidation nanolithography, Nanotechnology 21 (2010) 245301.

[37] Fu Y.Q, Colli A, Fasoli A, Luo J.K, Flewitt A.J, Ferrari A.C. and Milne W.I., Deep reactive ion etching as a tool for nanostructure fabrication, J. Vac. Sci. Technol. 27 (2009) 1520–1526.

[38] Li X. and Bohn P.W., Metal-assisted chemical etching in HF–H2O2 produces porous silicon, Appl. Phys. Lett. 77 (2000) 2572–2574.

[39] R.G. Mertens, K.B. Sundaram, Characterization of Silicon Nanowires Grown by Electroless Etching, Proceeding of the IEEE SoutheastCon 2012, Orlando, FL, DOI: 10.1109/SECon.2012.6196946.

[40] Baris Ozdemir, Mustafa Kulakci, Rasit Turan and Husnu Emrah Unalan, Effect of electroless etching parameters on the growth and reflection properties of silicon nanowires, Nanotechnology 22 (2011) 155606.

[41] Chen Chen, Rui Jia, Huihui Yue, Haofeng Li, Xinyu Liu, Degi Wu, Wuchang Ding, Tianchun Ye, Seiya Kasai, Hashizume Tamotsu, Junhao Chu, Shanli Wang, Silicon nanowire-array-textured solar cells for photovoltaic application, J. Appl. Phys, 108 (2010) 094318.

[42] B.R. Huang, Y.K. Yang, T.C. Lin, W.L. Yang, A simple and low-cost technique for silicon nanowire arrays based solar cells, Sol. Energy Mater Sol. Cells 98 (2012) 357-362.

[43] N. Megouda, T. Hadjersi, Y. Coffinier, S. Szunerits, R. Boukherroub, “Investigation of morphology, reflectance and photocatalytic activity of nanostructured silicon surfaces”, Microelectronic Engineering 159 (2016) 94–101.

[44] A. Smyrnakis, E. Almpanis, V. Constantoudis, N. Papanikolaou, E. Gogolides, "Optical properties of high aspect ratio plasma etched silicon nanowires: fabrication-induced variability dramatically reduces reflectance", Nanotechnology 26 (2015) 085301.

[45] R.G. Mertens, R.G. Blair, K.B. Sundaram, Recession and Characterization of Patterned Nanowires Grown by Electroless Etching of Silicon, ECS J. Solid State Sci. Technol. 1 (2012) 40-45.

[46] K. Peng, J. Hu, Y. Yan, Y. Wu, H. Fang, Y. Xu, S. Lee, and J. Zhu, Fabrication of Single-Crystalline Silicon Nanowires by Scratching a Silicon Surface with Catalytic Metal Particles, Adv. Funct. Mater. 16 (2006) 387–394.

[47] C. Riordan and R. Hulstrom, What is an air mass 1.5 spectrum?, IEEE. 0160-8371 (1990) 0000-1085. DOI: 10.1109/PVSC.1990.111784.

[48] A. S. Togonal, L. He, P. Roca, I. Cabarrocas, and Rusli, Effect of Wettability on the Agglomeration of Silicon Nanowire Arrays Fabricated by Metal-Assisted Chemical Etching, Langmuir, 2014, 30 (34), pp 10290–10298.

[49] D. Kumar, S. Srivastava, P. Singh, K. Sood, V. Singh, N. Dilawar and M. Husain. J. Nanopart. Res., 12. (2010) 2267.

[50] Srivastava S K, Kumar D, Singh P K, Kar M, Kumar V and Husain M Sol. Energy Mater. Sol. Cells 94 (2010) 1506–11.

[51] Ozdemir, B., Kulakci, M., Turan, R., Unalan, H.E., (2011) “Effect of electroless etching parameters on the growth and reflection properties of silicon nanowires”, *Nanotechnology,* 22: 155606/1-155606/7.

[52] M.E. Gurtin, A.I. Murdoch, “Surface stress in solids”, Int. J. Solids Struct. 14 (1978) 431–440.